Three distinct Holocene intervals of stalagmite deposition and non-deposition revealed in NW Madagascar, and their paleoclimate implications

Ny Riavo Gilbertinie Voarintsoa[1*†], Loren Bruce Railsback[1], George Albert Brook[2], Lixin Wang[2], Gayatri Kathayat[3], Hai Cheng[3,4], Xianglei Li[3], Richard Lawrence Edwards[4], Amos Fety Michel Rakotondrazafy[5], Marie Olga Madison Razanatseheno[5]

[1] Department of Geology, University of Georgia, Athens, GA 30602-2501 U.S.A.
[2] Department of Geography, University of Georgia, Athens, Georgia, 30602-2502 U.S.A.
[3] Institute of Global Environmental Change, Xi'an Jiaotong University, Xi'an, Shaanxi 710049, P.R. China
[4] Department of Earth Sciences, University of Minnesota, Minneapolis, Minnesota 55455, U.S.A.
[5] Mention Sciences de la Terre et de l'Environnement, Domaine Sciences et Technologie, University d'Antananarivo, Madagascar

*Correspondence to: Ny Riavo Voarintsoa (nv1@uga.edu or nyriavony@gmail.com)

†Current address: Institute of Earth Sciences, The Hebrew University in Jerusalem, A. Safra Campus, 91904, Jerusalem, Israel (nyriavo.voarintsoa@mail.huji.ac.il)

ABSTRACT

Petrographic features, mineralogy, and stable isotopes from two stalagmites, ANJB-2 and MAJ-5, respectively from Anjohibe and Anjokipoty Caves, allow distinction of three intervals of the Holocene in NW Madagascar. The Malagasy *early* Holocene (between c. 9.8 and 7.8 ka) and *late* Holocene (after c. 1.6 ka) intervals (MEHI and MLHI, respectively) record evidence of stalagmite deposition. The Malagasy *middle* Holocene interval (MMHI, between c. 7.8 ka and 1.6 ka) is marked by a depositional hiatus of c. 6500 years.

Deposition of these stalagmites indicates that the two caves were sufficiently supplied with water to allow stalagmite formation. This suggests that the MEHI and MLHI intervals may have been comparatively wet in NW Madagascar. In contrast, the long-term depositional hiatus during the MMHI implies it was relatively drier than the MEHI and the MLHI.

The alternating "wet/dry/wet" conditions during the Holocene may have been linked to the long-term migrations of the Inter-Tropical Convergence Zone (ITCZ). When the ITCZ's mean position is farther south, NW Madagascar experiences wetter conditions, such as during the MEHI

and MLHI, and when it moves north, NW Madagascar climate becomes drier, such as during the MMHI. A similar wet/dry/wet succession during the Holocene has been reported in neighboring locations, such as southeastern Africa. Beyond these three subdivisions, the records also suggest wet conditions around the cold 8.2 ka event, suggesting a causal relationship. However, additional Southern Hemisphere high–resolution data will be needed to confirm this.

1. Introduction

Although much is known about Holocene climate change worldwide (Mayewski et al., 2004; Wanner and Ritz, 2011; Wanner et al., 2011; 2015), high-resolution climate data for the Holocene period is still regionally limited in the Southern Hemisphere (SH) (e.g., Wanner et al., 2008; Marcott et al., 2013; Wanner et al., 2015), including Madagascar. This uneven distribution of data hinders our understanding of the spatio-temporal characteristics of Holocene climate change, and the forcings involved. For example, some forcings would have influenced the behavior of the Inter-Tropical Convergence Zone (ITCZ) as well as monsoonal responses in low- to mid-latitude regions (e.g., Wanner et al., 2015; Talento and Barreiro, 2016). In fact, Madagascar is ideally located to provide data on SH Holocene climate changes because of its location in Southwestern Indian Ocean and because it is seasonally visited by the ITCZ (Fig. 1a). Furthermore, a karst belt with caves extends from the north to the south of the island (Fig. 1c), crossing latitudinal climate belts, and this could potentially be a source of stalagmite data. Thus, Madagascar is a natural laboratory to study ITCZ dynamics over time. New records from Madagascar could fill gaps in paleoclimate datasets for the SH that might help refine paleoclimate simulations, and thus provide a better understanding of global circulation and land–atmosphere–ocean interactions during the Holocene.

In this paper, we present records of stable isotopes, petrography, mineralogy, variability of layer-specific width (or LSW) from stalagmites from Anjohibe and Anjokipoty caves. Stalagmites are used because of their potential to store significant climatic information (e.g., Fairchild and Baker, 2012, p. 9–10), and in Anjohibe Cave, recent studies have shown the replicability of paleoclimate records from stalagmites (e.g., Burns et al., 2016).

Two stalagmites were investigated, and these allowed us to characterize Holocene climate change in NW Madagascar. First, we developed a record of climate change using the stalagmite

proxy data. With a better understanding of Madagascar's paleoclimate, we then investigated possible drivers of tropical climate change to isolate the major factors controlling the hydrological cycle in NW Madagascar and surrounding regions during the Holocene.

2. Setting

2.1. Stalagmites and their setting

Stalagmites are secondary cave deposits that are $CaCO_3$ precipitates from cave dripwater. Calcium carbonate precipitation occurs mainly by CO_2 degassing, which increases the pH of the dripwater and thus increases the concentration of CO_3^{2-}. In some cases, evaporation may also contribute to increased Ca^{2+} and/or CO_3^{2-} concentrations in dripwater. CO_2 degassing occurs when high-PCO_2 water from the epikarst encounters low-PCO_2 cave air. Evaporation occurs when humidity inside the cave is relatively low. The fundamental equation for stalagmite deposition is:

$$Ca^{2+}_{(aq)} + 2HCO^{-}_{3\,(aq)} \rightleftharpoons CaCO_{3\,(s)} + CO_{2\,(g)} + H_2O_{(l)} \quad \text{(Eq. 1)}$$

Growth and non-growth of stalagmites depends on conditions that affect Eq. 1. An increase in Ca^{2+} drives the equation to the right (towards precipitation) and an increase in CO_2 of the cave air and/or H_2O drives it to the left (towards dissolution). All components of the equation are influenced by the supply of water to the cave, which is generally climate-dependent. More water enters the cave during warm/rainy seasons than during cold/dry seasons. Stalagmites will form when cave dripwater is saturated with respect to calcite and/or aragonite. If the water passes through the bedrock too quickly to dissolve significant carbonate rock, and/or enters the cave and reaches the stalagmite too quickly to degas significant CO_2, it will not be saturated with respect to $CaCO_3$, inhibiting stalagmite formation. Stalagmite growth will slow as dripwater declines and will stop entirely if flow ceases. Vegetation provides CO_2 to the soil via root respiration so the vegetation cover above the cave and the type of vegetation can promote or limit stalagmite growth. Overall, the karst hydrological system plays a crucial role in the deposition and non-deposition of stalagmites, and this is closely linked to changes in local and regional environment and climate.

2.2. Regional environmental setting

Stalagmites ANJB-2 and MAJ-5 were collected from Anjohibe and Anjokipoty caves, respectively, in the Majunga region of NW Madagascar (Fig. 1). Sediments and fossils from these caves have already provided many insights about the paleoenvironmental and archaeological history of NW Madagascar (e.g., Burney et al., 1997, 2004; Brook et al., 1999; Gommery et al., 2011; Jungers et al., 2008; Vasey et al., 2013; Burns et al., 2016; Voarintsoa et al., 2017b).

Anjohibe (S15° 32' 33.3"; E046° 53' 07.4") and Anjokipoty (S15° 34' 42.2"; E046° 44' 03.7") are about 16.5 km apart (Fig. 1c). Their location in the zone visited by the ITCZ (e.g., Nassor and Jury, 1998) makes them ideal sites to test the hypothesis that latitudinal migration of the ITCZ influenced the Holocene climate of NW Madagascar (e.g., Chiang and Bitz, 2005; Broccoli et al., 2006; Chiang and Friedman, 2012; Schneider et al., 2014). Majunga has a tropical savanna climate (Aw) according to the Köppen-Geiger climate classification, with a distinct wet summer (from October to April) and dry winter (May-September). The mean annual rainfall is around 1160 mm. The mean maximum temperature in November, the hottest month in the summer, is about 32°C. The mean minimum temperature in July, the coldest month of the dry winter, is about 18°C (Fig. 1b).

2.3. Climate of Madagascar

The climate of Madagascar is unique because of its varied topography and its position in the Indian Ocean (Figs. S1–S2; also see for e.g., Jury, 2003; DGM, 2008, Douglas and Zinke, 2015, p. 281-299; Voarintsoa et al., 2017b, p.138-139; Scroxton et al., 2017). Regionally distinct rainfall gradients from east to west and from north to south are evident across the country (Jury, 2003; Dewar and Richard, 2007), and these are linked to easterly trade winds in winter (May-October) and northwesterly tropical storms in summer, respectively. In NW Madagascar, summer rainfall is monsoonal and it is in phase with the seasonal southward migration of the ITCZ. Chiang and Bitz' (2005) and Broccoli et al.'s (2006)'s have suggested that cooler/warmer intervals bring the ITCZ south/north, thus regions in tropical SH are wet/dry. Generally, the ITCZ migrates towards the Earth's warmer hemisphere (Frierson and Hwang, 2012; Kang et al., 2008; McGee et al., 2014; Sachs et al., 2009). In fact, longer-term ITCZ migration appears to have affected climate in NW

Madagascar between c. 370 CE and 800 CE (see Fig, 8 of Voarintsoa et al., 2017b). This relationship was inferred from changes in global climate conditions.

The climate of Madagascar is also influenced by changes in Indian Ocean sea surface temperature (SST) (Zinke et al., 2004; see also Kunhert et al., 2014) and changes in SST the Aghulas Current off southwestern Madagascar (Lutjeharms, 2006; Beal et al., 2011; Zinke et al., 2014). The most immediate signal is the Indian Ocean Dipole (IOD), or Indian Ocean Zonal Mode (Li et al., 2003; Zinke et al., 2004), but El-Niño Southern Oscillation (ENSO) may also influence its climate (e.g., Brook et al., 1999). IOD has been linked to Holocene climate variability in tropical Indian Ocean (Abram et al., 2009; Tierney et al., 2013). However, its linkages to ENSO is still debated (e.g., Saji et al., 1999; Li et al., 2003; Lee et al., 2008; Brown et al., 2009; Schott et al., 2009; Shinoda et al., 2004; Venzke et al., 2000; Abram et al., 2008; Saji and Yagamata, 2003; Meyers et al., 2007). The complex interactions between these inter-annual climatic factors make them an ideal topic for further investigation using high-resolution records, and thus they will not be the focus of this paper. However, their possible effects are referred to briefly in Supplementary text no. 4.

2.4. The Holocene in NW Madagascar

Little is hitherto known about Holocene climate change in NW Madagascar nor about the major drivers of long-term climatic changes there. Most paleoclimate information from this region covers the last two millennia with more focus on the anthropogenic effects on the Malagasy ecosystems (e.g., Crowley and Samonds, 2013; Burns et al., 2016; Voarintsoa et al., 2017b). This is because several studies show that megafaunal extinctions in Madagascar coincide with the arrival of humans around 2-3 thousand (ka) BP (e.g., see Table 1 of Virah-Sawmy et al., 2010; MacPhee and Burney, 1991; Burney et al., 1997; Crowley, 2010). There are even fewer long-term paleoclimate records for the NW region, with only sediments from Lake Mitsinjo (3.5 ka BP; Matsumoto and Burney, 1994) and stalagmites from Anjohibe Cave (40 ka BP; Burney et al. 1997) providing records of more than 3 ka. Even though these records provide useful information about paleoenvironmental changes in NW Madagascar, links to global climatic changes, particularly the links to changes in ITCZ, are not yet fully understood.

3. Methods

3.1. Radiometric dating

A total of 22 samples were drilled from Stalagmite ANJB-2 and 9 samples for Stalagmite MAJ-5 for U-series dating (Table S1 and S2). Each sample is a long (~5 to 20 mm), narrow (~1-2mm), and shallow (~1 mm) trench, allowing us to extract 50–250 mg of $CaCO_3$ powder. We followed the chemical procedures described in Edwards et al. (1987) and Shen et al. (2002) when separating uranium and thorium. U/Th measurements were performed on the multi-collector ICP-MS of the University of Minnesota, USA and on a similar instrument in the Stable Isotopes Laboratory of Xi'an, in Jiaotong, China. Instrument details are provided in Cheng et al. (2013). Corrected ^{230}Th ages assume an initial $^{230}Th/^{232}Th$ atomic ratio of $4.4 \pm 2.2 \times 10^{-6}$. This is the ratio for "bulk earth" or crustal material at secular equilibrium with a $^{232}Th/^{238}U$ value of 3.8. The uncertainty in the "bulk earth" value is assumed to be ±50% (see footnotes to Tables S1 and S2). The error in the final "corrected age" incorporates this uncertainty. The radiometric data are reported as years BP, where BP is Before Present, and "Present" is A.D. 1950. Stalagmite chronologies were constructed using the StalAge1.0 algorithm of Scholz and Hoffman (2011) and Scholz et al. (2012), an algorithm using a Monte-Carlo simulation. The algorithm can identify major and minor outliers and age inversions. The StalAge scripts were run on the statistics program R version 3.2.2 (2015-08-14). The age models were adjusted considering hiatal surfaces identified in the samples, using the approach of Railsback et al. (2013; see their Fig. 9).

3.2. Petrography and mineralogy

Petrography and mineralogy of the two stalagmites were investigated 1) by examining both the polished surfaces and the scanned images of the sectioned stalagmites, and by identifying any diagenetic fabrics (e.g., Zhang et al., 2014) that could potentially affect stable isotope values, 2) by observing eleven oversized thin sections (3x2 in) under the Leitz Laborlux 12 Pol microscope and the Leica DMLP equipped with QCapture in the Sedimentary Geochemistry Lab at the University of Georgia, 3) by using scanning electron microscopy (SEM) to better understand the mineralogical fabrics at locations of interest (Fig. S13), and 4) by analyzing about 30–100 mg of powdered speleam layers (n=15) on a Bruker D8 X-ray Diffractometer in the Department of

177 Geology, University of Georgia. For calcite and aragonite identification, we used CoKα radiation at
178 a 2θ angle between 20° and 60°.
179 Layer-specific width (LSW) of clearly-defined layers was measured at selected locations on
180 the stalagmite polished surfaces (Fig. S4; Sletten et al., 2013; Railsback et al., 2014; Voarintsoa et
181 al., 2017b). LSW is the horizontal distance between two points on the flanks of the stalagmite
182 where convexity is greatest. It is the width near the top of the stalagmite when the layer being
183 examined was deposited. LSW is measured at right angles to the growth axis of the stalagmite; it
184 is the horizontal distance between two points on the layer growth surface, at which a virtual line
185 inclined at 35° to the growth axis becomes tangent to the layer growth surface as shown in Fig.
186 S4. LSW may vary along the length of the stalagmite, with smaller values suggesting drier
187 conditions and larger values wetter conditions.
188
189 3.3. Stable isotopes
190 Samples of 50–100 μg were drilled along the stalagmite's growth axis for stable isotope
191 analysis. The trench size is very small (1.5 x 0.5 x 0.5 mm). Since a small mixture of calcite and
192 aragonite could potentially change the $\delta^{18}O$ and $\delta^{13}C$ of the measured spelean layers (see for
193 example Frisia et al., 2002), drilling and sample extraction were carefully done on individually
194 discrete layers using the smallest drill-bit head (SSW-HP-1/4) to avoid potential mixing between
195 calcite and aragonite. The polished surface of the two stalagmites were examined to see if features
196 of diagenetic alteration are present (see for example fig. 2 of Zhang et al., 2014), but none was
197 found. During sampling, the mineralogy at the crest, where stable isotope samples were extracted,
198 was recorded for future mineralogical correction.
199 Aragonite oxygen and carbon isotopic corrections were performed to compensate for
200 aragonite's inherent fractionation of heavier isotopes (e.g., Romanek et al., 1992; Kim et al., 2007;
201 McMillan et al., 2005) and to remove the mineralogical bias in isotopic interpretation between
202 calcite and aragonite. The correction consists of subtracting 0.8‰ for $\delta^{18}O$ (Kim and O'Neil, 1997;
203 Tarutani et al., 1969; Kim et al., 2007; Zhang et al., 2014) and 1.7 ‰ for $\delta^{13}C$ (Rubinson and Clayton,
204 1969; Romanek et al., 1992) for the aragonite, as has been done previously (e.g., Holmgren et al.,

2003; Sletten et al., 2013; Liang et al., 2015; Railsback et al., 2016; Voarintsoa et al., 2017a), as shown in equations 2 and 3 below (where $R_{A/C}$ is the aragonite percentage if not 100%).

$$\delta^{18}O_{corr.}\ (‰, VPDB) = \delta^{18}O_{uncorr.}\ (‰, VPDB) - [R_{A/C} \times 0.8\ (‰, VPDB)] \quad \text{(Eq. 2)}$$

$$\delta^{13}C_{corr.}\ (‰, VPDB) = \delta^{13}C_{uncorr.}\ (‰, VPDB) - [R_{A/C} \times 1.7\ (‰, VPDB)] \quad \text{(Eq. 3)}$$

Supplementary Figures S6–S8 show both the corrected and uncorrected isotopic records.

For the analytical methods, oxygen and carbon isotope ratios were measured using the Finnigan MAT-253 mass spectrometer fitted with the Kiel IV Carbonate Device of the Xi'an Stable Isotope Laboratory in China (ANJB-2; n=654) and using the Delta V Plus at 50°C fitted with the GasBench-IRMS machine of the Alabama Stable Isotope Laboratory in USA (MAJ-5; n=286). Analytical procedures using the MAT 253 are identical to those described in Dykoski et al. (2005), with isotopic measurement errors of less than 0.1 ‰ for both $\delta^{13}C$ and $\delta^{18}O$. Analytical methods and procedures using the GasBench-IRMS machine are identical to those described in Skrzypek and Paul (2006), Paul and Skrzypek (2007), and Lambert and Aharon (2011), with ±0.1 ‰ errors for both $\delta^{13}C$ and $\delta^{18}O$. In both techniques, the results are reported relative to Vienna PeeDee Belemnite (VPDB) and with standardization relative to NBS19. An inter-lab comparison of the isotopic results was conducted, and it involved replicating every tenth sample of Stalagmite MAJ-5 at both labs. This exercise showed a strong correlation between the lab results (Fig. S5).

4. Results

4.1. Radiometric data

Results from radiometric analyses of the two stalagmites are presented in Tables S1 and S2. Corrected ^{230}Th ages suggest that Stalagmite ANJB-2 was deposited between c. 8977±50 and c. 161±64 years BP, and Stalagmite MAJ-5 was deposited between c. 9796±64 and c. 150±24 years BP. These ages collectively indicate stalagmite deposition at the beginning (between c. 9.8 and 7.8 ka BP) and at the end of the Holocene (after c. 1.6 ka BP). In both stalagmites, the older ages have small 2σ errors and they generally fall in correct stratigraphic order, except sample ANJB-2-120 and its replicate ANJB-2-120R, which were not used because of the sample's high porosity and high detritals content. In contrast, many of the younger ages have larger uncertainties. This is mainly because many of the younger samples have very low uranium concentration and the

detrital thorium concentration is also high, similar to what Dorale et al. (2004) reported. We also understand that the value for initial ^{230}Th correction, i.e. the initial ^{230}Th/^{232}Th atomic ratio of 4.4 ± 2.2 × 10^{-6} for a bulk earth with a ^{232}Th/^{238}U value of 3.8, in these samples could have slightly altered the ^{230}Th age of these younger samples, leading to larger uncertainties (such as discussed in Lachniet et al., 2012). We encountered similar problems while working on other younger samples from the same cave, but we compared the stable isotope profile with other published records using isochron dating methods, and results did not differ significantly (see Fig. 9 of Voarintsoa et al., 2017b). Since this work does not focus on decadal or centennial interpretation of the Late Holocene stable isotope data, additional chronology adjustment has not been made, and we used the chronology from StalAge to construct the time series. However, in Figures 5 and 6, age uncertainties are given below the stable isotope profiles so that comparisons with other records can accommodate these uncertainties.

The key finding from our age and petrographic data for the two stalagmites is that they indicate three distinct intervals of growth and non-growth during the Holocene (Figs. 2–4, 7). The evidence for this includes: (1) $CaCO_3$ deposition between c. 9.8 and 7.8 ka BP, (2) a long depositional hiatus between c. 7.8 and 1.6 ka BP, and (3) resumption of $CaCO_3$ deposition after c. 1.6 ka BP. In the rest of the paper, we will refer to these intervals as the Malagasy Early Holocene Interval (MEHI), Malagasy Mid-Holocene Interval (MMHI), and Malagasy Late Holocene Interval (MLHI), respectively.

4.2. Stable isotopes

Raw values of δ^{18}O and δ^{13}C for Stalagmite ANJB-2 range from –8.9 to –2.3‰ (mean = –5.0‰), and from –11.0 to +5.2‰ (mean = –4.2‰), respectively, relative to VPDB. Raw values of δ^{18}O and δ^{13}C for Stalagmite MAJ-5 range from –8.8 to –0.9‰ (mean = –4.9‰), and from –9.4 to +2.6‰ (mean = –4.4‰), respectively, relative to VPDB. Mean δ^{18}O and δ^{13}C values are distinguishable between the MEHI and the MLHI. In both stalagmites, the amplitude of δ^{18}O fluctuations was fairly constant throughout the Holocene; whereas the δ^{13}C records show a dramatic shift toward higher values (i.e. from -10.9‰ to +3.8‰, VPDB) at c. 1.5 ka BP.

The MEHI and MLHI are isotopically distinct (Fig. 4). The MEHI is characterized by statistically correlated $\delta^{18}O$ and $\delta^{13}C$ (r^2=0.65 and 0.53), and much depleted $\delta^{13}C$ values (c –11.0 to –4.0 ‰). A prominent isotopic excursion is evident between c. 8.1 and c. 8.3 ka BP (Fig. 5), when stalagmite $\delta^{18}O$ and $\delta^{13}C$ ratios reach their lowest values of –6.8 and –10.9‰, respectively. In contrast to the MEHI, the values of $\delta^{18}O$ and $\delta^{13}C$ during the MLHI are poorly correlated (r^2=0.25 and 0.17), and $\delta^{13}C$ values are more enriched (Figs. 4, 6). Since Stalagmites ANJB-2 and MAJ-5 were collected from two different caves, 16 km apart, it is not surprising to see discrepancies between the stable isotopes during similar intervals, suggesting that local karst conditions could be one of the discrepancy factors. Another potential source for the discrepancy is the larger uncertainty of the younger ages due to low uranium and high detrital concentrations. This U-Th aspect has been a challenge for several young stalagmites (e.g., Dorale et al., 2004; Lachniet et al., 2012) including samples from NW Madagascar (this study). While the utility of speleothems as a climate proxy largely depends on replication of stable isotope values, this study specifically highlights the replication of stalagmite deposition and non-deposition and the isotopic characteristics of each depositional intervals of the Holocene.

4.3. Mineralogy, petrography, and layer-specific width

In both stalagmites ANJB-2 and MAJ-5, the hiatus of deposition is characterized by a well-developed Type L surface (Figs. 2, 3, S15). Petrography and mineralogy are distinct before and after this hiatus (Figs. 3, 5–6). Below the hiatus, laminations are well preserved in both stalagmites. Above the hiatus, laminations are not well-preserved, although noted in some intervals.

In Stalagmite ANJB-2, LSW varies from 37 to 26.5 mm with a mean of 30 mm. It decreases to 28 mm at the hiatus (Fig. 3). The mineralogy is dominated by aragonite below the hiatus, although there are also a few thick layers of primary calcite. A thin (~2-3 mm) layer of white, very soft, and porous aragonite is identified just below the hiatus (Fig. S15). This layer is also calcite and aragonite, with calcite dominant, and the calcite layers contain macro-cavities that are mostly off-axis macroholes (Shtober-Zisu et al., 2012).

As noted in previous section (4.2), there is a prominent isotopic excursion at c. 8.2 ka BP, and this excursion is in the calcite layer in Stalagmite ANJB-2 at 195–202 mm from its top. X-ray

diffraction spectrum from this layer suggests that the mineralogy is 100% calcite (Figs. S14, S16–S17). We believe the calcite to be primary and not a diagenetic product of aragonite for three reasons. First, the laminations in the thick layer of calcite were not altered (Figs. S16–S17). Second, the polished surface of the stalagmite shows no evidence of fiber relicts and textural ghosts such as observed in Juxtlahuaca Cave in southwestern Mexico (Lachniet et al., 2012) and in Shennong Cave in southeastern China (Zhang et al., 2014). Third, petrographic comparison with known examples of primary and secondary calcite observed under microscope (e.g., Railsback, 2000; Perrin et al., 2014) suggests that there is no strong evidence of aragonite–to–calcite transformation.

In Stalagmite MAJ-5, LSW varies from 50 to 22 mm with a mean of 35.5 mm. It decreases to 22 mm at the hiatus (Fig. 3). Below the hiatus, mineralogy is an even mixture between calcite and aragonite. Above the hiatus, mineralogy is mainly calcite, except the uppermost 2 mm where mineralogy is 75% calcite and 25% aragonite. Macro-cavities are also present throughout this upper part of Stalagmite MAJ-5.

4.4. Summary of results

The various proxy climate records from Stalagmites ANJB-2 and MAJ-5 suggest three distinct climate/hydrological intervals during the Holocene. The MEHI (c. 9.8 to 7.8 ka BP), with evidence of stalagmite deposition, is characterized by statistically correlated $\delta^{18}O$ and $\delta^{13}C$ (r^2=0.65 and 0.53) and more negative $\delta^{13}C$ values (c. –11.0 to –4.0 ‰). The MMHI (c. 7.8 to 1.6 ka BP) is marked by a long-term hiatus in deposition, which is preceded by a well-developed Type L surface in both Stalagmite ANJB-2 and MAJ-5 (Figs. 3, S15). The Type L surface is observed as an upward narrowing of stalagmite width and layer thickness. It is best developed in Stalagmite MAJ-5 (Fig. S15). In Stalagmite ANJB-2, the hiatus at the Type L surface is additionally preceded by a c. 3 mm thick layer of highly porous, very soft, and fibrous white crystals of aragonite (the only aragonite with such properties). This aragonite is topped by a thin and well-defined layer of detrital materials (Fig. S15), further evidence of a hiatus. Finally, the MLHI (after c. 1.6 ka BP) is characterized by poorly correlated $\delta^{18}O$ and $\delta^{13}C$ (r^2=0.25–0.17), and by a marked shift toward higher $\delta^{13}C$ values (Figs. 4, 6).

5. Discussion

5.1. Paleoclimate significance of stalagmite growth and non-growth: implications for paleohydrology

Growth and non-growth of stalagmites depends on several factors linked to water availability, which is largely determined by climate (more water during warm/rainy seasons and less water during cold/dry seasons). Water is the main dissolution and transporting agent for most chemicals in speleothems. Cave hydrology varies significantly over time in response to climate, and this variability influences the formation or dissolution of $CaCO_3$. In this regard, calcium carbonate does not form if there is little or no water entering the cave, or if there is too much (see Sect. 2.1). Absence of groundwater recharge most typically occurs during extremely dry conditions, whereas excessive water input to the cave occurs during extremely wet conditions. In the latter scenario, water is undersaturated and flow rates are too fast to allow degassing. Often, water availability is reflected in the extent of vegetation above and around the cave, as plants require soil moisture or shallow groundwater to survive and propagate, and this contributes to the stalagmites' processes of formation. The link between stalagmite growth/non-growth and cave dripwater and soil CO_2 is broadly influenced by changes in climate.

Major hiatuses in stalagmite deposition could be marked by a variety of features, including the presence of erosional surfaces, chalkification, dirt bands/detrital layers, offsetting of the growth axis, and/or sometimes by color changes (e.g., Holmgren et al., 1995; Dutton et al., 2009; Railsback et al., 2013; Railsback et al., 2015; Voarintsoa et al., 2017a). Railsback et al. (2013) were able to identify significant features in stalagmites that allow distinction between non-deposition during extremely wet (Type E surfaces) and non-deposition during extremely dry conditions (Type L surfaces; Fig. 3). Physical properties of stalagmites that are evidence of extreme dry and wet events are summarized in Table 1 of Railsback et al. (2013) and the mechanisms are explained in their Figure 5.

Type E surfaces are layer-bounding surfaces between two spelean layers when the underlying layers show evidence of truncation. The truncation results from dissolution or erosion (thus the name "E") of previously-formed stalagmites layers by abundant undersaturated water.

Type E surfaces are commonly capped with a layer of calcite (Railsback et al., 2013). This mineralogical trend is not surprising as calcite commonly forms under wetter conditions (e.g., Murray, 1954; Pobeguin, 1965; Siegel, 1965; Thrailkill, 1971; Cabrol and Coudray, 1982; Railsback et al. 1994; Frisia et al., 2002). Additionally, non-carbonate detrital materials are commonly abundant with varying grain size (i.e., from silt- to sand-size; Railsback et al., 2013).

Type L surfaces, on the other hand, are layer-bounding surfaces where the layers become narrower upward and thinner towards the flanks of the stalagmite. Decreases in layer thickness and stalagmites width upward are indications of lessening deposition (thus the name "L"; Railsback et al., 2013). Aragonite is a very common mineralogy below a Type L surface, especially in warmer settings. Layers of aragonite commonly form under drier conditions (Murray, 1954; Pobeguin, 1965; Siegel, 1965; Thrailkill, 1971; Cabrol and Coudray, 1982; Railsback et al., 1994; Frisia et al., 2002). Non-carbonate detrital materials are scarce, and if present, they tend to form a very thin horizon of very fine dust material (Railsback et al., 2013). Identification of Type L surfaces is aided by measuring the LSW (e.g., Sletten et al., 2013; Railsback et al., 2014; Fig. S4).

5.2. Holocene climate in NW Madagascar

The age models and petrographic features of Stalagmites ANJB-2 and MAJ-5 suggest three distinct Holocene climate intervals (MEHI, MMHI, and MLHI; see Sect. 4.1) in NW Madagascar. Possible conditions during these intervals are illustrated in the sketches of Figure 4.

5.2.1. Malagasy early Holocene interval (c. 9.8 –7.8 ka BP)

Stalagmite deposition during the early Holocene suggests that the chambers where stalagmites ANJB-2 and MAJ-5 were collected were sufficiently supplied with water to allow $CaCO_3$ precipitation, in accord with Eq.1. This in turn implies relatively wet conditions that could indicate longer summer rainy seasons relative to modern climate, or wet years in NW Madagascar. The correlative $\delta^{13}C$ and $\delta^{18}O$ values further suggest that vegetation consistently responded to changes in moisture availability, which in turn was dependent on climate.

The prominent negative $\delta^{18}O$ and $\delta^{13}C$ excursions in Stalagmite ANJB-2 (Sect. 4.2; Figs. 5 and 10) are parallel to the $\delta^{18}O$ excursion of the Greenland ice core records at c. 8.2 ka BP (e.g.

Alley et al., 1997). The decrease in $\delta^{18}O$ and $\delta^{13}C$ values and the presence of calcite mineralogy at the same interval combine to suggest a wet 8.2 ka BP event in NW Madagascar. The 8.2 ka BP event was triggered by a release of freshwater from the melting Laurentide Ice Sheet into the North Atlantic basin, bringing cooler conditions in several NH regions (e.g., Alley et al., 1997; Barber et al., 1999), and via global teleconnections, this may have affected climate in NW Madagascar (see Sect. 5.5).

The MEHI terminated when conditions became much drier, as suggested by increasing $\delta^{18}O$ and $\delta^{13}C$ values in Stalagmite ANJB-2, by decreasing LSW in both stalagmites, and by the presence of a major Type L surfaces in both stalagmites. The thin (c. 3 mm), porous, and white aragonite layer in Stalagmite ANJB-2, a very similar deposit to that described in Niggemann et al. (2003), suggests that the terminal drought was at times severe. Aragonite is a $CaCO_3$ polymorph that forms preferentially under drier conditions (Murray, 1954; Pobeguin, 1965; Siegel, 1965; Thrailkill, 1971; Cabrol and Coudray, 1982; Railsback et al. 1994; Frisia et al., 2002). The porous aragonite layer in Stalagmite ANJB-2 is capped by a very thin layer of non-carbonate, brown detritus, which may have been transported to the stalagmite as an aerosol and accumulated on the dry stalagmite surface over time. Accumulation of the detritus must take place in the absence of dripwater (e.g., Railsback et al., 2013). A shift to drier conditions is also supported by isotopic data from Stalagmite ANJ94-5 from Anjohibe Cave (Wang and Brook, 2013; Wang, 2016) in which relatively low $\delta^{13}C$ and $\delta^{18}O$ values prior to 7.6 ka BP give way to episodically greater values thereafter.

5.2.2. Malagasy mid-Holocene interval (c. 7.8–1.6 ka BP)

The MMHI was a long (~6.5 ka) depositional hiatus in both stalagmites (Figs. 2–3), potentially suggesting dry conditions. The question is why did neither stalagmite grow during the MMHI? Here, we try to explain the factors and the climatic conditions that may have been responsible.

The documented severe dry conditions at the end of the MEHI (see Sect. 5.2.1) could have had a significant influence (1) on the cave hydrological system (e.g., Fig. 5 of Asrat et al., 2007; Bosák, 2010), such as the water conduits (primary or secondary porosity) to the chambers, and (2) on the vegetation cover above the caves, particularly above the chambers where Stalagmites

ANJB-2 and MAJ-5 were collected. On one hand, it is possible that the dry conditions late in the MEHI could not only bring lesser water recharge to the cave, but also lowered the hydraulic head, and increased the rate of evapo-transpiration in the vadose zone. This condition possibly allowed more air to penetrate the aquifer, perhaps enhancing prior carbonate precipitation (PCP) in pores and conduits above the caves (e.g., Fairchild and McMillan, 2007; Fairchild et al., 2000; Johnson et al., 2006; Karmann et al., 2007; McDonald et al., 2007). This process must have blocked water moving towards Stalagmites ANJB-2 and MAJ-5. On the other hand, the late MEHI drying trend (Sect. 5.2.1) could have challenged vegetation to grow, and we assume that some areas above Anjohibe and Anjokipoty caves must have been devoid of vegetation. Consequently, biomass activities could have been reduced. Because vegetation contributes CO_2 to the carbonic acid dissolving $CaCO_3$, its absence in certain areas above the cave could decrease the pH of the percolating water, and perhaps dissolution did not occur. Under these conditions, even if water reached the stalagmites, it may not have precipitated carbonate.

Whatever factors were responsible for the long term-depositional hiatus in Stalagmite ANJB-2 and MAJ-5, we believe that the hiatus was caused by disturbances to water catchments that feed the chambers at Anjohibe and Anjokipoty caves. The disturbances could be inherited from the very dry conditions at the end of the MEHI, and/or due to the lack of water supply, perhaps associated with an increase in epikarst ventilation, and/or by the absence of vegetation. Water and vegetation are two components of the karst system that play an important role in $CaCO_3$ dissolution and precipitation (see Eq. 1). Their disturbance may have limited limestone dissolution in the epikarst and then carbonate precipitation in the cave zone.

Other evidence supports the idea of at least episodic dryness during the MMHI. A work on a 2-meter long stalagmite (ANJ94-5) from Anjohibe Cave suggests episodic dryness during the MMHI and a depositional hiatus around the time when Stalagmites ANJB-2 and MAJ-5 stopped growing (Wang and Brook, 2013; Wang, 2016). For regional comparison, dry spells were also felt in Central and Southeastern Madagascar (e.g., Gasse and Van Campo, 1998; Virah-Sawmy et al., 2009).

In summary, several lines of evidence suggest relatively drier climate in NW Madagascar during the MMHI compared to the MEHI. Drier intervals generally imply drier summer seasons

with less rainfall (Fig. 8), perhaps reflecting shorter visits by the ITCZ. In this regard, even though the region received rainfall, the necessary conditions could not have been attained to activate the growth of Stalagmites ANJB-2 and MAJ-5, thus the hiatuses.

5.2.3. Malagasy Late Holocene Interval (c. 1.6 ka BP–present)

Resumption of stalagmite deposition after c. 1.6 ka BP suggests a wetter climate in NW Madagascar with reactivation of the previous epikarst hydrologic system. Climatic conditions must have been similar to those of the early Holocene. The sudden beginning of stalagmite growth during the MLHI and the large $\delta^{13}C$ shift from depleted to enriched values at c. 1.5 ka BP (Fig. 6), after such long hiatuses may have been associated with changes in vegetation cover above the cave linked to human activities (e.g., Burns et al., 2016; Crowley and Samonds, 2013; Crowther et al., 2016; Voarintsoa et al., 2017b). Lower $\delta^{13}C$ values in Stalagmite MAJ-5 after 0.8 ka BP (Fig. 3), compared to higher values in Stalagmite ANJB-2, may suggest different local karst conditions, either natural, human-induced, or something else, at each site. Further investigations will be necessary to better understand this.

5.3. Holocene climate in NW Madagascar: implications for ITCZ dynamics

In NW Madagascar, stalagmite deposition during the MEHI and the MLHI suggests there was sufficient dripwater for stalagmite growth and therefore wetter conditions. This may indicate a more southerly mean position of the ITCZ. Factors that could influence the mean position of the ITCZ include changes in insolation (e.g., Haug et al., 2001; Wang et al., 2005; Cruz et al., 2005; Fleitmann et al., 2003, 2007; Schefuß et al., 2005; Suziki, 2011; Kutzbach and Liu, 1997; Partridge et al., 1997; Verschuren et al., 2009; Voarintsoa et al., 2017a) and difference in temperature between the two hemispheres (e.g., Chiang and Bitz, 2005; Broccoli et al., 2006; Chiang and Friedman, 2012; Kang et al., 2008; McGee et al., 2014; Talento and Barreiro, 2016).

In contrast, the depositional hiatuses during the MMHI could suggest overall drier conditions, and thus a northward migration of the mean ITCZ. It may agree with the paleoclimate simulation of Braconnot et al. (2007), although the simulation is of shorter term than the MMHI hiatus, but additional paleoclimate records are needed to improve its spatial and temporal

resolution. A northward shift in the mean position of the ITCZ is consistent with drier conditions in the southern tropics, e.g., weaker South American Summer Monsoon (Cruz et al., 2005; Seltzer et al., 2000; Wang et al., 2007; but see also Fig. 9 of Zhang et al., 2013), and with wetter conditions in the northern tropics (e.g., Dykoski et al., 2005; Fleitmann et al., 2007; Gasse, 2000; Haug et al., 2001; Weldeab et al., 2007; Zhang et al., 2013).

5.4. Regional comparisons

Records from neighboring locations (Figs. 8–9; Table S3) show that the Holocene wet/dry/wet succession reported here for NW Madagascar also affected other locations. For example, hydrogen isotope compositions of the n-C31 alkane in GeoB9307-3 from a 6.51 m long marine sediment core retrieved about 100 km off the Zambezi delta show a similar wet/dry/wet climate during Early, Middle, and Late Holocene respectively (Schefuß et al., 2011). These changes correspond to changes in temperature from ~26.5° to 27.25° to 27°C, respectively, in the Mozambique Channel, as suggested by alkenone SST records from sediment cores MD79257 (Bard et al., 1997; Sonzogni et al., 1998). The Zambezi catchment is specifically relevant here because it is located at the southern boundary of the modern ITCZ, and so has a similar climatic setting as NW Madagascar, and its sensitivity to the latitudinal migration of the ITCZ could parallel that of Madagascar. Likewise, temperature reconstruction from the Mozambique Channel could be used to link regional changes in paleorainfall with regional changes in temperature. A general overview of the Holocene climate in the African neighboring locations to Madagascar suggests a roughly consistent wetter and drier climate during the early and middle Holocene, respectively (Fig. 9, Table S3, also see Gasse, 2000; Singarayer and Burrough, 2015). However, Late Holocene paleoclimate reconstructions vary. A simple explanation to this Late Holocene variability is unlikely, but several interacting factors, including the latitudinal migration of the ITCZ, changes in ocean oscillations and sea surface temperatures, volcanic aerosols, and anthropogenic influences may have played a role (e.g., Nicholson, 1996; Gasse, 2000; Tierney et al., 2008; Truc et al., 2013). Assessing these factors is beyond the scope of this study.

5.5. The 8.2 ka BP event in Madagascar: linkage to ITCZ and AMOC

The 8.2 ka BP event, a widespread cold event in the NH (e.g., Alley et al., 1997), is apparent in the stalagmite records (Figs. 5, 10). Stalagmite ANJB-2 $\delta^{18}O$ and $\delta^{13}C$ ratios reach their lowest values of –6.8 and –10.9‰, respectively during that interval, and mineralogy is primary calcite. These proxies suggest wet interval in NW Madagascar.

The 8.2 ka event was triggered by an abrupt freshwater influx from the melting Laurentide Ice Sheet into the North Atlantic (Alley et al., 1997; Barber et al., 1999; Kleiven et al., 2008; Carlson et al., 2008; Renssen et al, 2010; Wiersma et al., 2011; Wanner et al., 2015). This influx of meltwater altered the density and salinity of the NADW (e.g., Thornalley et al., 2009), weakening the Atlantic Meridional Overturning Circulation (AMOC, e.g., Barber et al., 1999; Clark et al., 2001; Daley et al., 2011; Vellinga and Wood 2002; Dong and Sutton 2002, 2007; Dahl et al. 2005; Zhang and Delworth 2005; Daley et al., 2011; Renssen et al., 2001). Weakening of the AMOC would cause a widespread cooling in the NH regions (e.g., Clark et al., 2001; Thomas et al., 2007) but warming in the SH regions (Wiersma et al., 2011; Wiersma and Renssen, 2006), creating a "bipolar seesaw" effect (e.g., Crowley, 1992; Broecker, 1998). The interhemispheric temperature difference between the NH and SH from this effect may be the driver of the southward displacement of the mean position of the ITCZ during the 8.2 ka abrupt cooling event. This may have intensified the Malagasy monsoon in NW Madagascar during austral summers, similar to what happened to the South American Summer Monsoon in Brazil (e.g., Cheng et al., 2009). In contrast, regions in the NH monsoon regions became drier at 8.2 ka BP as the Asian Monsoon and the East Asian Monsoon weakened (e.g., Wang et al., 2005; Dykoski et al., 2005; Cheng et al., 2009; Liu et al., 2013). The cold NH climate conditions and the wet climate conditions in NW Madagascar at 8.2 ka BP (Fig. 10) could suggest causal relationships. However, further research and data will be needed to confirm this possibility.

6. Conclusions

Petrography, mineralogy, and stable isotope records from Stalagmite ANJB-2, from Anjohibe Cave, and Stalagmite MAJ-5, from Anjokipoty Cave, combine to suggest three distinct intervals of changing climate in Madagascar during the Holocene: relatively wet conditions during the MEHI,

relatively drier conditions, possibly due to episodic dry intervals, during the MMHI, and relatively wet conditions during the MLHI. The timing of stalagmite deposition during the MEHI and the MLHI in NW Madagascar could be attributed to a more southward migration and/or an expanded ITCZ, increasing the duration of the summer rainy seasons, perhaps linked to a stronger Malagasy monsoon. This could have been tied to the temperature gradient between the two hemispheres and weakening of the AMOC. In contrast, the c. 6500–year depositional hiatus during the MMHI could indicate a northward migration of the ITCZ, leading to relatively drier conditions in NW Madagascar. The evidence of the 8.2 ka event in the Malagasy records may further suggest a close link between paleoenvironmental changes in Madagascar and abrupt climatic events in the NH, suggesting that during the MEHI Madagascar's climate was very sensitive to abrupt ocean-atmosphere events in the NH.

Although the ITCZ is unquestionably one of the climatic drivers influencing climate in Madagascar and surrounding locations, several climatic factors need to be investigated in more detail. For example, we do not fully understand if the latitudinal migration is paired with the expansion and/or contraction of the ITCZ, which would affect the strengths of the associated monsoon systems. In addition, the interplay between ITCZ and other factors involving changes in sea surface temperatures, particularly IOD-ENSO, needs to be investigated in details. Data-model comparison (for example at the 8.2 ka event) and improved spatial and temporal resolution of paleoclimate datasets could be an approach to address this challenge.

Author Contribution

N.R.G.V. conceived the research and experiments. N.R.G.V, G.K, A.F.M.R, and M.O.M.R did the fieldwork and collected the samples. X.L., G.K., H.C., R.L.E, and N.R.G.V contributed to the ^{230}Th dating analyses. N.R.G.V provided detailed investigation of the two stalagmites, provided stable isotope measurements, prepared thin sections, and conducted X-ray diffraction and SEM analyses on the samples. G.K. also assisted with the isotopic measurements on Stalagmite ANJB-2. N.R.G.V. wrote the first draft of the manuscript and led the writing. L.B.R. and G.A.B. provided a thorough review of the draft. N.R.G.V. and L.B.R. discussed and revised the manuscript, with additional comments from L.W. N.R.G.V revised the paper with input from all authors, reviewers, and editors.

551 Data availability: Data for this paper are available at xxxxxxxxx

552

553 Competing Interests. The authors declare no conflict of interest.

554

555 Special issue statement. This article is a part of the special issue "Southern perspectives on climate
556 and the environment from the Last Glacial Maximum through the Holocene: the Southern
557 Hemisphere Assessment of PalaeoEnvironments (SHAPE) project". It was presented at the "SHAPE
558 International Focus Group Workshop: Southern Hemisphere climate of the present and past"
559 workshop in Santiago Chile on November 2-4, 2016.

560 Acknowledgments. This work was supported by grants from (1) the National Natural Science
561 Foundation of China (NSFC 41230524, NBRP 2013CB955902, and NSFC 41472140) to Hai Cheng
562 and Gayatri Kathayat, (2) the Geological Society of America Research Grant (GSA 11166-16) and
563 John Montagne Fund Award to N. Voarintsoa, (3) the Miriam Watts-Wheeler Graduate Student
564 Grant from the Department of Geology at UGA to N. Voarintsoa, and (4) the International
565 Association of Sedimentology Post-Graduate Grant to N. Voarintsoa. We also thank the
566 Schlumberger Foundation for providing additional support to N. Voarintsoa's research. We thank
567 the Department of Geology at the University of Antananarivo, in Madagascar, the Ministry of
568 Energy and Mines, the local village and guides in Majunga for easing our research in Madagascar.
569 We specifically thank Dr. Voahangy Ratrimo, former Department Head of the Department of
570 Geology at the University of Antananarivo, for collaborating with us and for giving us permission
571 to conduct field expedition in Madagascar. We thank Prof. Paul Schroeder for giving us access to
572 use the X-ray diffractometer of the Geology Department to conduct analysis on the mineralogy of
573 the two stalagmites. We thank Prof. John Shields of the Georgia Electron Microscope, University
574 of Georgia, for giving Voarintsoa access to use the Zeiss 1450EP (Carl Zeiss, Inc., Thornwood, NY)
575 for SEM purposes. We also thank Prof. Sally Walker for allowing us to use the microscope of the
576 paleontology lab and for helping us to photograph the stalagmites at very high resolution. We also
577 thank Prof. John Chiang of the University of California at Berkeley, for sharing his thoughts and
578 guiding us to literature of relevance to this study.

579

Edited by: Nerilie Abram

Reviewed by: two anonymous referees

References

Abram, N. J., McGregor, H. V., Gagan, M. K., Hantoro, W. S., and Suwargadi, B. W.: Oscillations in the southern extent of the Indo-Pacific Warm Pool during the mid-Holocene, Quaternary Sci Rev, 28, 2794-2803, Doi 10.1016/J.Quascirev.2009.07.006, 2009.

Abram, N. J., Gagan, M. K., Cole, J. E., Hantoro, W. S., and Mudelsee, M.: Recent intensification of tropical climate variability in the Indian Ocean, Nature Geosci, 1, 849-853, 2008.

Alley, R. B., Mayewski, P. A., Sowers, T., Stuiver, M., Taylor, K. C., and Clark, P. U.: Holocene climatic instability: A prominent, widespread event 8200 yr ago, Geology, 25, 483-486, 1997.

Asrat, A., Baker, A., Mohammed, M. U., Leng, M. J., Van Calsteren, P., and Smith, C.: A high-resolution multi-proxy stalagmite record from Mechara, Southeastern Ethiopia: palaeohydrological implications for speleothem palaeoclimate reconstruction, J Quaternary Sci, 22, 53-63, Doi 10.1002/Jqs.1013, 2007.

Barber, D. C., Dyke, A., Hillaire-Marcel, C., Jennings, A. E., Andrews, J. T., Kerwin, M. W., Bilodeau, G., McNeely, R., Southon, J., Morehead, M. D., and Gagnon, J. M.: Forcing of the cold event of 8,200 years ago by catastrophic drainage of Laurentide lakes, Nature, 400, 344-348, Doi 10.1038/22504, 1999.

Bard, E., Rostek, F., and Sonzogni, C.: Interhemispheric synchrony of the last deglaciation inferred from alkenone palaeothermometry, Nature, 385, 707-710, Doi 10.1038/385707a0, 1997.

Beal, L. M., De Ruijter, W. P. M., Biastoch, A., Zahn, R., and 136, S. W. I. W. G.: On the role of the Agulhas system in ocean circulation and climate, Nature, 472, 429-436, Doi 10.1038/Nature09983, 2011.

Bosák, P.: Dating of processes in karst and caves: implication for show caves presentation, 6th ISCA Congress Proceedings, Slovakia, 2011, 34-41, 2011.

Braconnot, P., Otto-Bliesner, B., Harrison, S., Joussaume, S., Peterchmitt, J. Y., Abe-Ouchi, A., Crucifix, M., Driesschaert, E., Fichefet, T., Hewitt, C. D., Kageyama, M., Kitoh, A., Laine, A., Loutre, M. F., Marti, O., Merkel, U., Ramstein, G., Valdes, P., Weber, S. L., Yu, Y., and Zhao,

608 Y.: Results of PMIP2 coupled simulations of the Mid-Holocene and Last Glacial Maximum -
609 Part 1: experiments and large-scale features, Clim Past, 3, 261-277, 2007.
610 Broccoli, A. J., Dahl, K. A., and Stouffer, R. J.: Response of the ITCZ to Northern Hemisphere cooling,
611 Geophys Res Lett, 33, 10.1029/2005gl024546, 2006.
612 Broecker, W. S.: Paleocean circulation during the Last Deglaciation: A bipolar seesaw?,
613 Paleoceanography, 13, 119-121, 10.1029/97PA03707, 1998.
614 Brook, G. A., Rafter, M. A., Railsback, L. B., Sheen, S. W., and Lundberg, J.: A high-resolution proxy
615 record of rainfall and ENSO since AD 1550 from layering in stalagmites from Anjohibe Cave,
616 Madagascar, Holocene, 9, 695-705, Doi 10.1191/095968399677907790, 1999.
617 Brown, J., Lynch, A. H., and Marshall, A. G.: Variability of the Indian Ocean Dipole in coupled model
618 paleoclimate simulations, J Geophys Res-Atmos, 114, 10.1029/2008jd010346, 2009.
619 Burney, D. A., Burney, L. P., Godfrey, L. R., Jungers, W. L., Goodman, S. M., Wright, H. T., and Jull,
620 A. J. T.: A chronology for late prehistoric Madagascar, Journal of Human Evolution, 47, 25-
621 63, Doi 10.1016/J.Jhevol.2004.05.005, 2004.
622 Burney, D. A., James, H. F., Grady, F. V., Rafamantanantsoa, J. G., Ramilisonina, Wright, H. T., and
623 Cowart, J. B.: Environmental change, extinction and human activity: evidence from caves
624 in NW Madagascar, Journal of Biogeography, 24, 755-767, 10.1046/J.1365-
625 2699.1997.00146.X, 1997.
626 Burns, S. J., Godfrey, L. R., Faina, P., McGee, D., Hardt, B., Ranivoharimanana, L., and Randrianasy,
627 J.: Rapid human-induced landscape transformation in Madagascar at the end of the first
628 millennium of the Common Era, Quaternary Sci Rev, 134, 92-99,
629 10.1016/j.quascirev.2016.01.007, 2016.
630 Cabrol, P., and Coudray, J.: Climatic fluctuations influence the genesis and diagenesis of carbonate
631 speleothems in southwestern France, National Speleological Society Bulletin 44, 112-117,
632 1982.
633 Carlson, A. E., Legrande, A. N., Oppo, D. W., Came, R. E., Schmidt, G. A., Anslow, F. S., Licciardi, J.
634 M., and Obbink, E. A.: Rapid early Holocene deglaciation of the Laurentide ice sheet, Nat
635 Geosci, 1, 620-624, 10.1038/ngeo285, 2008.

636 Cheng, H., Edwards, R. L., Shen, C. C., Polyak, V. J., Asmerom, Y., Woodhead, J., Hellstrom, J., Wang,
637 Y. J., Kong, X. G., Spotl, C., Wang, X. F., and Alexander, E. C.: Improvements in Th-230 dating,
638 Th-230 and U-234 half-life values, and U-Th isotopic measurements by multi-collector
639 inductively coupled plasma mass spectrometry, Earth Planet Sc Lett, 371, 82-91, Doi
640 10.1016/J.Epsl.2013.04.006, 2013.
641 Cheng, H., Fleitmann, D., Edwards, R. L., Wang, X. F., Cruz, F. W., Auler, A. S., Mangini, A., Wang, Y.
642 J., Kong, X. G., Burns, S. J., and Matter, A.: Timing and structure of the 8.2 kyr BP event
643 inferred from delta O-18 records of stalagmites from China, Oman, and Brazil, Geology, 37,
644 1007-1010, Doi 10.1130/G30126a.1, 2009.
645 Chiang, J. C. H., and Bitz, C. M.: Influence of high latitude ice cover on the marine Intertropical
646 Convergence Zone, Clim Dynam, 25, 477-496, 10.1007/s00382-005-0040-5, 2005.
647 Chiang, J. C. H., and Friedman, A. R.: Extratropical Cooling, Interhemispheric Thermal Gradients,
648 and Tropical Climate Change, Annual Review of Earth and Planetary Sciences, 40, 383-412,
649 10.1146/Annurev-Earth-042711-105545, 2012.
650 Clark, P. U., Marshall, S. J., Clarke, G. K. C., Hostetler, S. W., Licciardi, J. M., and Teller, J. T.:
651 Freshwater Forcing of Abrupt Climate Change During the Last Glaciation, Science, 293, 283-
652 287, 10.1126/science.1062517, 2001.
653 Crowley, B. E., and Samonds, K. E.: Stable carbon isotope values confirm a recent increase in
654 grasslands in northwestern Madagascar, The Holocene, 23, 1066-1073, Doi
655 10.1177/0959683613484675, 2013.
656 Crowley, B. E.: A refined chronology of prehistoric Madagascar and the demise of the megafauna,
657 Quaternary Sci Rev, 29, 2591-2603, Doi 10.1016/J.Quascirev.2010.06.030, 2010.
658 Crowley, T. J.: North Atlantic Deep Water cools the southern hemisphere, Paleoceanography, 7,
659 489-497, 10.1029/92PA01058, 1992.
660 Crowther, A., Lucas, L., Helm, R., Horton, M., Shipton, C., Wright, H. T., Walshaw, S., Pawlowicz,
661 M., Radimilahy, C., Douka, K., Picornell-Gelabert, L., Fuller, D. Q., and Boivin, N. L.: Ancient
662 crops provide first archaeological signature of the westward Austronesian expansion, P
663 Natl Acad Sci USA, 113, 6635-6640, 10.1073/pnas.1522714113, 2016.

664 Cruz, F. W., Burns, S. J., Karmann, I., Sharp, W. D., Vuille, M., Cardoso, A. O., Ferrari, J. A., Dias, P.
665 L. S., and Viana, O.: Insolation-driven changes in atmospheric circulation over the past
666 116,000 years in subtropical Brazil, Nature, 434, 63-66, Doi 10.1038/Nature03365., 2005.
667 Dahl, K., Broccoli, A., and Stouffer, R.: Assessing the role of North Atlantic freshwater forcing in
668 millennial scale climate variability: a tropical Atlantic perspective, Clim Dynam, 24, 325-
669 346, 10.1007/s00382-004-0499-5, 2005.
670 Daley, T. J., Thomas, E. R., Holmes, J. A., Street-Perrott, F. A., Chapman, M. R., Tindall, J. C., Valdes,
671 P. J., Loader, N. J., Marshall, J. D., Wolff, E. W., Hopley, P. J., Atkinson, T., Barber, K. E.,
672 Fisher, E. H., Robertson, I., Hughes, P. D. M., and Roberts, C. N.: The 8200yr BP cold event
673 in stable isotope records from the North Atlantic region, Global Planet Change, 79, 2011.
674 Dewar, R. E., and Richard, A. F.: Evolution in the hypervariable environment of Madagascar, P Natl
675 Acad Sci USA, 104, 13723-13727, 10.1073/pnas.0704346104, 2007.
676 DGM [Direction Générale de la Météorologie]: Le changement climatique à Madagascar. 2008.
677 Dong, B. W., and Sutton, R. T.: Adjustment of the coupled ocean-atmosphere system to a sudden
678 change in the Thermohaline Circulation, Geophys Res Lett, 29, 2002.
679 Dong, B., and Sutton, R. T.: Enhancement of ENSO variability by a weakened Atlantic thermohaline
680 circulation in a coupled GCM, J Climate, 20, 4920-4939, 10.1175/Jcli4284.1, 2007.
681 Dorale, J. A., Edwards, R. L., Alexander, E. C., Shen, C.-C., Richards, D. A., and Cheng, H.: Uranium-
682 Series Dating of Speleothems: Current Techniques, Limits, & Applications, in: Studies of
683 Cave Sediments: Physical and Chemical Records of Paleoclimate, edited by: Sasowsky, I. D.,
684 and Mylroie, J., Springer US, Boston, MA, 177-197, 2004.
685 Douglass, K., and Zinke, J.: Forging Ahead By Land and By Sea: Archaeology and Paleoclimate
686 Reconstruction in Madagascar, Afr Archaeol Rev, 32, 267-299, 10.1007/s10437-015-9188-
687 5, 2015.
688 Dutton, A., Bard, E., Antonioli, F., Esat, T. M., Lambeck, K., and McCulloch, M. T.: Phasing and
689 amplitude of sea-level and climate change during the penultimate interglacial, Nat Geosci,
690 2, 355-359, 10.1038/Ngeo470, 2009.
691 Dykoski, C. A., Edwards, R. L., Cheng, H., Yuan, D. X., Cai, Y. J., Zhang, M. L., Lin, Y. S., Qing, J. M.,
692 An, Z. S., and Revenaugh, J.: A high-resolution, absolute-dated Holocene and deglacial

693 Asian monsoon record from Dongge Cave, China, Earth Planet Sc Lett, 233, 71-86,
694 10.1016/j.epsl.2005.01.036, 2005.
695 Edwards, R. L., Chen, J. H., and Wasserburg, G. J.: U-238 U-234-Th-230-Th-232 Systematics and the
696 Precise Measurement of Time over the Past 500000 Years, Earth Planet Sc Lett, 81, 175-
697 192, 1987.
698 Fairchild, I. J., and Baker, A.: Speleothem Science: From Processes to Past Environments, edited
699 by: Bradley, R., Wiley-Blackwell, 2012.
700 Fairchild, I. J., and McMillan, E. A.: Speleothems as indicators of wet and dry periods, International
701 Journal of Speleology, 36, 69-74, 2007.
702 Fairchild, I. J., Borsato, A., Tooth, A. F., Frisia, S., Hawkesworth, C. J., Huang, Y. M., McDermott, F.,
703 and Spiro, B.: Controls on trace element (Sr-Mg) compositions of carbonate cave waters:
704 implications for speleothem climatic records, Chem Geol, 166, 255-269, Doi
705 10.1016/S0009-2541(99)00216-8, 2000.
706 Fleitmann, D., Burns, S. J., Mangini, A., Mudelsee, M., Kramers, J., Villa, I., Neff, U., Al-Subbary, A.
707 A., Buettner, A., Hippler, D., and Matter, A.: Holocene ITCZ and Indian monsoon dynamics
708 recorded in stalagmites from Oman and Yemen (Socotra), Quaternary Sci Rev, 26, 170-188,
709 10.1016/J.Quascirev.2006.04.012, 2007.
710 Fleitmann, D., Burns, S. J., Mudelsee, M., Neff, U., Kramers, J., Mangini, A., and Matter, A.:
711 Holocene forcing of the Indian monsoon recorded in a stalagmite from Southern Oman,
712 Science, 300, 1737-1739, Doi 10.1126/Science.1083130, 2003.
713 Frierson, D. M. W., and Hwang, Y. T.: Extratropical Influence on ITCZ Shifts in Slab Ocean
714 Simulations of Global Warming, J Climate, 25, 720-733, 10.1175/Jcli-D-11-00116.1, 2012.
715 Frisia, S., Borsato, A., Fairchild, I. J., McDermott, F., and Selmo, E. M.: Aragonite–calcite
716 relationships in speleothems (Grotte de Clamouse, France): environment, fabrics, and
717 carbonate geochemistry., J Sediment Res, 772, 687-699, 2002.
718 Garcin, Y., Vincens, A., Williamson, D., Guiot, J., and Buchet, G.: Wet phases in tropical southern
719 Africa during the last glacial period, Geophys Res Lett, 33, 10.1029/2005GL025531, 2006.

720 Gasse, F., and Van Campo, E.: A 40,000-yr pollen and diatom record from Lake Tritrivakely,
721 Madagascar, in the southern tropics, Quaternary Res, 49, 299-311, Doi
722 10.1006/Qres.1998.1967, 1998.
723 Gasse, F.: Hydrological changes in the African tropics since the Last Glacial Maximum, Quaternary
724 Sci Rev, 19, 189-211, Doi 10.1016/S0277-3791(99)00061-X, 2000.
725 Gommery, D., Ramanivosoa, B., Faure, M., Guerin, C., Kerloc'h, P., Senegas, F., and
726 Randrianantenaina, H.: Oldest evidence of human activities in Madagascar on subfossil
727 hippopotamus bones from Anjohibe (Mahajanga Province), Cr Palevol, 10, 271-278,
728 10.1016/j.crpv.2011.01.006, 2011.
729 Haug, G. H., Hughen, K. A., Sigman, D. M., Peterson, L. C., and Rohl, U.: Southward migration of
730 the intertropical convergence zone through the Holocene, Science, 293, 1304-1308, Doi
731 10.1126/Science.1059725, 2001.
732 Head, M. J., and Gibbard, P. L.: Formal subdivision of the Quaternary System/Period: Past, present,
733 and future, Quatern Int, 383, 4-35, 10.1016/j.quaint.2015.06.039, 2015.
734 Holmgren, K., Karlen, W., and Shaw, P. A.: Paleoclimatic Significance of the Stable Isotopic
735 Composition and Petrology of a Late Pleistocene Stalagmite from Botswana, Quaternary
736 Res, 43, 320-328, DOI 10.1006/qres.1995.1038, 1995.
737 Holmgren, K., Lee-Thorp, J. A., Cooper, G. R. J., Lundblad, K., Partridge, T. C., Scott, L., Sithaldeen,
738 R., Talma, A. S., and Tyson, P. D.: Persistent millennial-scale climatic variability over the past
739 25,000 years in Southern Africa, Quaternary Sci Rev, 22, 2311-2326, 10.1016/S0277-
740 3791(03)00204-X, 2003.
741 Johnson, K. R., Hu, C. Y., Belshaw, N. S., and Henderson, G. M.: Seasonal trace-element and stable-
742 isotope variations in a Chinese speleothem: The potential for high-resolution
743 paleomonsoon reconstruction, Earth Planet Sc Lett, 244, 394-407,
744 10.1016/j.epsl.2006.01.064, 2006.
745 Jungers, W. L., Demes, B., and Godfrey, L. R.: How big were the "Giant" extinct lemurs of
746 Madagascar?, in: Elwyn Simons: A search for origins, edited by: Fleagle, J. G., and Gilbert,
747 C. G., Springer, New York, 343-360, 2008.

748 Jury, M. R.: The Climate of Madagascar, in: The Natural History of Madagascar, edited by:
749 Goodman, S. M., and Benstead, J. P., Chicago: Universtity of Chicago, 75-87, 2003.
750 Kang, S. M., Held, I. M., Frierson, D. M. W., and Zhao, M.: The response of the ITCZ to extratropical
751 thermal forcing: Idealized slab-ocean experiments with a GCM, J Climate, 21, 3521-3532,
752 10.1175/2007jcli2146.1, 2008.
753 Karmann, I., Cruz, F. W., Viana, O., and Burns, S. J.: Climate influence on geochemistry parameters
754 of waters from Santana-Perolas cave system, Brazil, Chem Geol, 244, 232-247,
755 10.1016/j.chemgeo.2007.06.029, 2007.
756 Kim, S. T., O'Neil, J. R., Hillaire-Marcel, C., and Mucci, A.: Oxygen isotope fractionation between
757 synthetic aragonite and water: Influence of temperature and Mg2+ concentration,
758 Geochim Cosmochim Ac, 71, 4704-4715, 10.1016/J.Gca.2007.04.019, 2007.
759 Kim, S.-T., and O'Neil, J. R.: Equilibrium and nonequilibrium oxygen isotope effects in synthetic
760 carbonates, Geochim Cosmochim Ac, 61, 3461-3475, doi.org/10.1016/S0016-
761 7037(97)00169-5, 1997.
762 Kleiven, H. F., Kissel, C., Laj, C., Ninnemann, U. S., Richter, T. O., and Cortijo, E.: Reduced North
763 Atlantic Deep Water coeval with the glacial Lake Agassiz freshwater outburst, Science, 319,
764 60-64, 10.1126/science.1148924, 2008.
765 Konecky, B. L., Russell, J. M., Johnson, T. C., Brown, E. T., Berke, M. A., Werne, J. P., and Huang, Y.
766 S.: Atmospheric circulation patterns during late Pleistocene climate changes at Lake
767 Malawi, Africa, Earth Planet Sc Lett, 312, 318-326, 10.1016/j.epsl.2011.10.020, 2011.
768 Kuhnert, H., Kuhlmann, H., Mohtadi, M., Meggers, H., Baumann, K. H., and Patzold, J.: Holocene
769 tropical western Indian Ocean sea surface temperatures in covariation with climatic
770 changes in the Indonesian region, Paleoceanography, 29, 423-437,
771 10.1002/2013pa002555, 2014.
772 Kutzbach, J. E., and Liu, Z.: Response of the African Monsoon to Orbital Forcing and Ocean
773 Feedbacks in the Middle Holocene, Science, 278, 440, 1997.
774 Lachniet, M. S., Bernal, J. P., Asmerom, Y., and Polyak, V.: Uranium loss and aragonite-calcite age
775 discordance in a calcitized aragonite stalagmite, Quat Geochronol, 14, 26-37,
776 10.1016/j.quageo.2012.08.003, 2012.

777 Lambert, W. J., and Aharon, P.: Controls on dissolved inorganic carbon and delta C-13 in cave
778 waters from DeSoto Caverns: Implications for speleothem delta C-13 assessments,
779 Geochim Cosmochim Ac, 75, 753-768, 10.1016/j.gca.2010.11.006, 2011.
780 Lee, T., and McPhaden, M. J.: Decadal phase change in large-scale sea level and winds in the Indo-
781 Pacific region at the end of the 20th century, Geophys Res Lett, 35,
782 10.1029/2007gl032419, 2008.
783 Li, T., Wang, B., Chang, C. P., and Zhang, Y. S.: A theory for the Indian Ocean dipole-zonal mode, J
784 Atmos Sci, 60, 2119-2135, 10.1175/1520-0469(2003)060<2119:Atftio>2.0.Co;2, 2003.
785 Liang, F., Brook, G. A., Kotlia, B. S., Railsback, L. B., Hardt, B., Cheng, H., Edwards, R. L., and
786 Kandasamy, S.: Panigarh cave stalagmite evidence of climate change in the Indian Central
787 Himalaya since AD 1256: Monsoon breaks and winter southern jet depressions,
788 Quaternary Sci Rev, 124, 145-161, 2015.
789 Liu, Z., Kutzbach, J., and Wu, L.: Modeling climate shift of El Nino variability in the Holocene,
790 Geophys Res Lett, 27, 2265-2268, 10.1029/2000GL011452, 2000.
791 Lutjeharms, J. R. E.: The Aghulas Current, Springer, 2006.
792 MacPhee, R. D. E., and Burney, D. A.: Dating of Modified Femora of Extinct Dwarf Hippopotamus
793 from Southern Madagascar - Implications for Constraining Human Colonization and
794 Vertebrate Extinction Events, J Archaeol Sci, 18, 695-706, Doi 10.1016/0305-
795 4403(91)90030-S, 1991.
796 Marcott, S. A., Shakun, J. D., Clark, P. U., and Mix, A. C.: A Reconstruction of Regional and Global
797 Temperature for the Past 11,300 Years, Science, 339, 1198, 2013.
798 Matsumoto, K., and Burney, D. A.: Late Holocene environments at Lake Mitsinjo, northwestern
799 Madagascar, The Holocene, 4, 16-24, 1994.
800 Mayewski, P. A., Rohling, E. E., Stager, J. C., Karlen, W., Maasch, K. A., Meeker, L. D., Meyerson, E.
801 A., Gasse, F., van Kreveld, S., Holmgren, K., Lee-Thorp, J., Rosqvist, G., Rack, F.,
802 Staubwasser, M., Schneider, R. R., and Steig, E. J.: Holocene climate variability, Quaternary
803 Res, 62, 243-255, Doi 10.1016/J.Yqres.2004.07.001, 2004.

McDonald, J., Drysdale, R., Hill, D., Chisari, R., and Wong, H.: The hydrochemical response of cave drip waters to sub-annual and inter-annual climate variability, Wombeyan Caves, SE Australia, Chem Geol, 244, 605-623, 2007.

McGee, D., Donohoe, A., Marshall, J., and Ferreira, D.: Changes in ITCZ location and cross-equatorial heat transport at the Last Glacial Maximum, Heinrich Stadial 1, and the mid-Holocene, Earth Planet Sc Lett, 390, 69-79, 10.1016/J.Epsl.2013.12.043, 2014.

McMillan, E. A., Fairchild, I. J., Frisia, S., Borsato, A., and McDermott, F.: Annual trace element cycles in calcite-aragonite speleothems: evidence of drought in the western Mediterranean 1200-1100 yr BP, J Quaternary Sci, 20, 423-433, 10.1002/jqs.943, 2005.

Meyers, G., McIntosh, P., Pigot, L., and Pook, M.: The Years of El Niño, La Niña, and Interactions with the Tropical Indian Ocean, J Climate, 20, 2872-2880, 10.1175/JCLI4152.1, 2007.

Middleton, J., and Middleton, V.: Karst and caves of Madagascar, Cave and Karst Science, 29, 13-20, 2002.

Murray, J. W.: The deposition of calcite and aragonite in caves., J Geol, 62, 481-492, 1954.

Nassor, A., and Jury, M. R.: Intra-seasonal climate variability of Madagascar. Part 1: Mean summer conditions, Meteorol Atmos Phys, 65, 31-41, Doi 10.1007/Bf01030267, 1998.

Nicholson, S.E.: Environmental change within the historical period, in: The Physical Geography of Africa, Goudie, A.S., Adams, W.M., Orme, A. (Eds.), Oxford University Press, Oxford, 60–75, 1996.

Niggemann, S., Mangini, A., Mudelsee, M., Richter, D. K., and Wurth, G.: Sub-Milankovitch climatic cycles in Holocene stalagmites from Sauerland, Germany, Earth Planet Sc Lett, 216, 539-547, Doi 10.1016/S0012-821x(03)00513-2, 2003.

Partridge, T. C., Demenocal, P. B., Lorentz, S. A., Paiker, M. J., and Vogel, J. C.: Orbital forcing of climate over South Africa: A 200,000-year rainfall record from the Pretoria saltpan, Quaternary Sci Rev, 16, 1125-1133, 1997.

Paul, D., and Skrzypek, G.: Assessment of carbonate-phosphoric acid analytical technique performed using GasBench II in continuous flow isotope ratio mass spectrometry, Int J Mass Spectrom, 262, 180-186, 10.1016/j.ijms.2006.11.006, 2007.

832 Perrin, C., Prestimonaco, L., Servelle, G., Tilhac, R., Maury, M., and Cabrol, P.: Aragonite–calcite
833 speleothems: identifying original and diagenetic features, J Sediment Res, 84, 245-269,
834 2014.
835 Pobeguin, T.: Sur les concrétions calcaires observés dans la Grotte de Moulis (Ariège), Société
836 Géologique de la France, Compte Rendus, 241, 1791-1793, 1965.
837 Railsback, L. B., Akers, P. D., Wang, L. X., Holdridge, G. A., and Voarintsoa, N. R.: Layer-bounding
838 surfaces in stalagmites as keys to better paleoclimatological histories and chronologies,
839 International Journal of Speleology, 42, 167-180, 10.5038/1827-806x.42.3.1, 2013.
840 Railsback, L. B., Brook, G. A., Chen, J., Kalin, R., and Fleisher, C. J.: Environmental Controls on the
841 Petrology of a Late Holocene Speleothem from Botswana with annual layers of aragonite
842 and calcite, J Sediment Res A, 64, 147-155, 1994.
843 Railsback, L. B., Brook, G. A., Ellwood, B. B., Liang, F., Cheng, H., and Edwards, R. L.: A record of wet
844 glacial stages and dry interglacial stages over the last 560kyr from a standing massive
845 stalagmite in Carlsbad Cavern, New Mexico, USA, Palaeogeography, Palaeoclimatology,
846 Palaeoecology, 438, 256-266, http://dx.doi.org/10.1016/j.palaeo.2015.08.010, 2015.
847 Railsback, L. B., Brook, G. A., Liang, F., Marais, E., Cheng, H., and Edwards, R. L.: A multi-proxy
848 stalagmite record from northwestern Namibia of regional drying with increasing global-
849 scale warmth over the last 47kyr: The interplay of a globally shifting ITCZ with regional
850 currents, winds, and rainfall, Palaeogeography, Palaeoclimatology, Palaeoecology, 461,
851 109-121, 2016.
852 Railsback, L. B., Xiao, H. L., Liang, F. Y., Akers, P. D., Brook, G. A., Dennis, W. M., Lanier, T. E., Tan,
853 M., Cheng, H., and Edwards, R. L.: A stalagmite record of abrupt climate change and
854 possible Westerlies-derived atmospheric precipitation during the Penultimate Glacial
855 Maximum in northern China, Palaeogeogr Palaeocl, 393, 30-44, Doi
856 10.1016/J.Palaeo.2013.10.013, 2014.
857 Railsback, L.B.: Atlas of speleothem microfabrics.Available at. www.gly.uga.edu/
858 railsback/speleoatlas/SAindex1.html, 2000.

Renssen, H., Goosse, H., Fichefet, T., and Campin, J. M.: The 8.2 kyr BP event simulated by a Global Atmosphere—Sea-Ice—Ocean Model, Geophys Res Lett, 28, 1567-1570, 10.1029/2000GL012602, 2001.

Renssen, H., Goosse, H., Crosta, X., and Roche, D. M.: Early Holocene Laurentide Ice Sheet deglaciation causes cooling in the high-latitude Southern Hemisphere through oceanic teleconnection, Paleoceanography, 25, PA3204, doi10.1029/2009pa001854, 2010.

Romanek, C. S., Grossman, E. L., and Morse, J. W.: Carbon Isotopic Fractionation in Synthetic Aragonite and Calcite - Effects of Temperature and Precipitation Rate, Geochim Cosmochim Ac, 56, 419-430, Doi 10.1016/0016-7037(92)90142-6, 1992.

Rubinson, M., and Clayton, R. N.: Carbon-13 fractionation between aragonite and calcite, Geochim Cosmochim Ac, 33, 997-1002, 1969.

Sachs, J. P., Sachse, D., Smittenberg, R. H., Zhang, Z., Battisti, D. S., and Golubic, S.: Southward movement of the Pacific intertropical convergence zone AD[thinsp]1400-1850, Nature Geosci, 2, 519-525, 2009.

Saint-Ours, J. D.: Les phénomènes karstiques à Madagascar, Annales de Spéléologie, 14, 275-291, 1959.

Saji, N. H., and Yamagata, T.: Possible impacts of Indian Ocean Dipole mode events on global climate, Clim Res, 25, 151-169, Doi 10.3354/Cr025151, 2003.

Saji, N. H., Goswami, B. N., Vinayachandran, P. N., and Yamagata, T.: A dipole mode in the tropical Indian Ocean, Nature, 401, 360-363, 10.1038/43855, 1999.

Schefuß , E., Kuhlmann, H., Mollenhauer, G., Prange, M., and Patzold, J.: Forcing of wet phases in southeast Africa over the past 17,000 years, Nature, 480, 509-512, DOI 10.1038/nature10685, 2011.

Schefuß, E., Schouten, S., and Schneider, R. R.: Climatic controls on central African hydrology during the past 20,000[thinsp]years, Nature, 437, 1003-1006, 2005.

Schneider, T., Bischoff, T., and Haug, G. H.: Migrations and dynamics of the intertropical convergence zone, Nature, 513, 45-53, 10.1038/Nature13636, 2014.

Scholz, D., and Hoffmann, D. L.: StalAge - An algorithm designed for construction of speleothem age models, Quat Geochronol, 6, 369-382, 10.1016/j.quageo.2011.02.002, 2011.

888 Scholz, D., Hoffmann, D. L., Hellstrom, J., and Ramsey, C. B.: A comparison of different methods
889 for speleothem age modelling, Quat Geochronol, 14, 94-104,
890 10.1016/j.quageo.2012.03.015, 2012.
891 Schott, F. A., Xie, S. P., and McCreary, J. P.: Indian Ocean Circulation and Climate Variability, Rev
892 Geophys, 47, 10.1029/2007rg000245, 2009.
893 Scroxton, N., Burns, S. J., McGee, D., Hardt, B., Godfrey, L. R., Ranivoharimanana, L., and Faina, P.:
894 Hemispherically in-phase precipitation variability over the last 1700 years in a Madagascar
895 speleothem record, Quaternary Sci Rev, 164, 25-36, 10.1016/j.quascirev.2017.03.017,
896 2017.
897 Seltzer, G., Rodbell, D., and Burns, S. J.: Isotopic evidence for Late Glacial and Holocene hydrologic
898 change in tropical South America. Geology, 28, 35-38, 2000.
899 Shen, C.-C., Lawrence Edwards, R., Cheng, H., Dorale, J. A., Thomas, R. B., Bradley Moran, S.,
900 Weinstein, S. E., and Edmonds, H. N.: Uranium and thorium isotopic and concentration
901 measurements by magnetic sector inductively coupled plasma mass spectrometry, Chem
902 Geol, 185, 165-178, 2002.
903 Shinoda, T., Alexander, M. A., and Hendon, H. H.: Remote Response of the Indian Ocean to
904 Interannual SST Variations in the Tropical Pacific, J Climate, 17, 362-372, 10.1175/1520-
905 0442(2004)017<0362:RROTIO>2.0.CO;2, 2004.
906 Shtober-Zisu, N., Schwarcz, H. P., Konyer, N., Chow, T., and Noseworthy, M. D.: Macroholes in
907 stalagmites and the search for lost water, J Geophys Res-Earth, 117, F03020, Doi
908 10.1029/2011jf002288, 2012.
909 Siegel, F. R.: Aspects of calcium carbonate deposition in Great Onyx Cave, Kentucky,
910 Sedimentology, 4, 285–299, 1965.
911 Singarayer, J. S., and Burrough, S. L.: Interhemispheric dynamics of the African rainbelt during the
912 late Quaternary, Quaternary Sci Rev, 124, 48-67, 2015.
913 Skrzypek, G., and Paul, D.: Delta C-13 analyses of calcium carbonate: comparison between the
914 GasBench and elemental analyzer techniques, Rapid Commun Mass Sp, 20, 2915-2920,
915 10.1002/rcm.2688, 2006.

916 Sletten, H. R., Railsback, L. B., Liang, F. Y., Brook, G. A., Marais, E., Hardt, B. F., Cheng, H., and
917 Edwards, R. L.: A petrographic and geochemical record of climate change over the last 4600
918 years from a northern Namibia stalagmite, with evidence of abruptly wetter climate at the
919 beginning of southern Africa's Iron Age, Palaeogeogr Palaeocl, 376, 149-162, Doi
920 10.1016/J.Palaeo.2013.02.030, 2013.
921 Sonzogni, C., Bard, E., and Rostek, F.: Tropical sea-surface temperatures during the last glacial
922 period: a view based on alkenones in Indian Ocean sediments, Quaternary Sci Rev, 17,
923 1185-1201, http://dx.doi.org/10.1016/S0277-3791(97)00099-1, 1998.
924 Stuiver, M., Reimer, P. J., Bard, E., Beck, J. W., Burr, G. S., Hughen, K. A., Kromer, B., McCormac,
925 G., Van der Plicht, J., and Spurk, M.: INTCAL98 radiocarbon age calibration, 24,000-0 cal
926 BP, Radiocarbon, 40, 1041-1083, 1998.
927 Suzuki, T.: Seasonal variation of the ITCZ and its characteristics over central Africa, Theor Appl
928 Climatol, 103, 39-60, 10.1007/s00704-010-0276-9, 2011.
929 Talento, S., and Barreiro, M.: Simulated sensitivity of the tropical climate to extratropical thermal
930 forcing: tropical SSTs and African land surface, Clim Dynam, 47, 1091-1110,
931 10.1007/s00382-015-2890-9, 2016.
932 Tarutani, T., Clayton, R. N., and Mayeda, T. K.: The effect of polymorphism and magnesium
933 substitution on oxygen isotope fractionation between calcium carbonate and water,
934 Geochim Cosmochim Ac, 33, 987-996, http://dx.doi.org/10.1016/0016-7037(69)90108-2,
935 1969.
936 Thomas, D. S. G., Bailey, R., Shaw, P. A., Durcan, J. A., and Singarayer, J. S.: Late Quaternary
937 highstands at Lake Chilwa, Malawi: Frequency, timing and possible forcing mechanisms in
938 the last 44ka, Quaternary Sci Rev, 28, 526-539, 2009.
939 Thomas, E. R., Wolff, E. W., Mulvaney, R., Steffensen, J. P., Johnsen, S. J., Arrowsmith, C., White, J.
940 W. C., Vaughn, B., and Popp, T.: The 8.2ka event from Greenland ice cores, Quaternary Sci
941 Rev, 26, 70-81, http://dx.doi.org/10.1016/j.quascirev.2006.07.017, 2007.
942 Thornalley, D. J. R., Elderfield, H., and McCave, I. N.: Holocene oscillations in temperature and
943 salinity of the surface subpolar North Atlantic, Nature, 457, 711-714,
944 10.1038/nature07717, 2009.

945 Thrailkill, J.: Carbonate Deposition in Carlsbad Caverns, J Geol, 79, 683-695, 1971.
946 Tierney, J. E., Smerdon, J. E., Anchukaitis, K. J., and Seager, R.: Multidecadal variability in East
947 African hydroclimate controlled by the Indian Ocean, Nature, 493, 389-392, 2013.
948 Tierney, J. E., and deMenocal, P. B.: Abrupt Shifts in Horn of Africa Hydroclimate Since the Last
949 Glacial Maximum, Science, 342, 843, 2013.
950 Tierney, J. E., Russell, J. M., and Huang, Y.: A molecular perspective on Late Quaternary climate
951 and vegetation change in the Lake Tanganyika basin, East Africa, Quaternary Sci Rev, 29,
952 787-800, http://dx.doi.org/10.1016/j.quascirev.2009.11.030, 2010.
953 Tierney, J. E., Russell, J. M., Huang, Y., Damsté, J. S. S., Hopmans, E. C., and Cohen, A. S.: Northern
954 Hemisphere Controls on Tropical Southeast African Climate During the Past 60,000 Years,
955 Science, 322, 252, 2008.
956 Truc, L., Chevalier, M., Favier, C., Cheddadi, R., Meadows, M. E., Scott, L., Carr, A. S., Smith, G. F.,
957 and Chase, B. M.: Quantification of climate change for the last 20,000years from
958 Wonderkrater, South Africa: Implications for the long-term dynamics of the Intertropical
959 Convergence Zone, Palaeogeography, Palaeoclimatology, Palaeoecology, 386, 575-587,
960 2013.
961 Vasey, N., Burney, D. A., and Godfrey, L.: Coprolites associated with Archaeolemur remains in
962 North-western Madagascar suggest dietary diversity and cave use in a subfossil prosimian,
963 in: Leaping Ahead: Advances in Prosimian Biology, edited by: Masters, J., Gamba, M., and
964 Génin, F., Springer, New York, NY, 149–156, 2013.
965 Vellinga, M., and Wood, R. A.: Global climatic impacts of a collapse of the Atlantic thermohaline
966 circulation, Climatic Change, 54, 251-267, Doi 10.1023/A:1016168827653, 2002.
967 Venzke, S., Latif, M., and Villwock, A.: The Coupled GCM ECHO-2, J Climate, 13, 1371-1383,
968 10.1175/1520-0442(2000)013<1371:TCGE>2.0.CO;2, 2000.
969 Verschuren, D., Sinninghe Damste, J. S., Moernaut, J., Kristen, I., Blaauw, M., Fagot, M., and Haug,
970 G. H.: Half-precessional dynamics of monsoon rainfall near the East African Equator,
971 Nature, 462, 637-641, 2009.
972 Vinther, B. M., Buchardt, S. L., Clausen, H. B., Dahl-Jensen, D., Johnsen, S. J., Fisher, D. A., Koerner,
973 R. M., Raynaud, D., Lipenkov, V., Andersen, K. K., Blunier, T., Rasmussen, S. O., Steffensen,

974 J. P., and Svensson, A. M.: Holocene thinning of the Greenland ice sheet, Nature, 461, 385-
975 388, 10.1038/nature08355, 2009.
976 Virah-Sawmy, M., Willis, K. J., and Gillson, L.: Evidence for drought and forest declines during the
977 recent megafaunal extinctions in Madagascar, Journal of Biogeography, 37, 506-519, Doi
978 10.1111/J.1365-2699.2009.02203.X, 2010.
979 Virah-Sawmy, M., Willis, K. J., and Gillson, L.: Threshold response of Madagascar's littoral forest to
980 sea-level rise, Global Ecol Biogeogr, 18, 98-110, 10.1111/j.1466-8238.2008.00429.x, 2009.
981 Voarintsoa, N. R. G., Brook, G. A., Liang, F. Y., Marais, E., Hardt, B., Cheng, H., Edwards, R. L., and
982 Railsback, L. B.: Stalagmite multi-proxy evidence of wet and dry intervals in northeastern
983 Namibia: Linkage to latitudinal shifts of the Inter-Tropical Convergence Zone and changing
984 solar activity from AD 1400 to 1950, The Holocene, 27, 384-396,
985 10.1177/0959683616660170, 2017a.
986 Voarintsoa, N.R.G., Wang, L., Bruce Railsback, L., Brook, G.A., Liang, F., Cheng, H., Lawrence
987 Edwards, R.: Multiple proxy analyses of a U/Th-dated stalagmite to reconstruct
988 paleoenvironmental changes in northwestern Madagascar between 370 CE and 1300 CE.
989 Palaeogeography, Palaeoclimatology, Palaeoecology 469, 138-155, 2017b.
990 Walker, M. J. C., Berkelhammer, M., Bjorck, S., Cwynar, L. C., Fisher, D. A., Long, A. J., Lowe, J. J.,
991 Newnham, R. M., Rasmussen, S. O., and Weiss, H.: Formal subdivision of the Holocene
992 Series/Epoch: a Discussion Paper by a Working Group of INTIMATE (Integration of ice-core,
993 marine and terrestrial records) and the Subcommission on Quaternary Stratigraphy
994 (International Commission on Stratigraphy), J Quaternary Sci, 27, 649-659,
995 10.1002/jqs.2565, 2012.
996 Wang, L.: Late Quaternary paleoenvironmental changes in Southern Africa and Madagascar:
997 evidence from aeolian, fluvial, and cave deposits, Unpub dissertation. University of
998 Georgia, Athens, Georgia, 312pp, 2016.
999 Wang, L., and Brook, G.A., 2013. Holocene Climate Changes in Northwest Madagascar: Evidence
1000 From a Two-meter-long Stalagmite From the Anjohibe Cave, Meeting Program of the
1001 Association of American Geographers, Published Online. Session 1512: Paleorecords of our

1002 Changing Earth I: Climate History and Human-Environment Interaction in the Old and New
1003 World Tropics, 2013.
1004 Wang, X., Auler, A. S., Edwards, R. L., Cheng, H., Ito, E., Wang, Y., Kong, X., and Solheid, M.:
1005 Millennial-scale precipitation changes in southern Brazil over the past 90,000 years,
1006 Geophys Res Lett, 34, n/a-n/a, 10.1029/2007GL031149, 2007.
1007 Wang, Y. J., Cheng, H., Edwards, R. L., He, Y. Q., Kong, X. G., An, Z. S., Wu, J. Y., Kelly, M. J., Dykoski,
1008 C. A., and Li, X. D.: The Holocene Asian monsoon: Links to solar changes and North Atlantic
1009 climate, Science, 308, 854-857, 10.1126/science.1106296, 2005.
1010 Wanner, H., and Ritz, S. P.: A web-based Holocene Climate Atlas (HOCLAT):
1011 http://www.oeschger.unibe.ch/research/projects/holocene_atlas/, 2011.
1012 Wanner, H., Beer, J., Butikofer, J., Crowley, T. J., Cubasch, U., Fluckiger, J., Goosse, H., Grosjean,
1013 M., Joos, F., Kaplan, J. O., Kuttel, M., Muller, S. A., Prentice, I. C., Solomina, O., Stocker, T.
1014 F., Tarasov, P., Wagner, M., and Widmann, M.: Mid- to Late Holocene climate change: an
1015 overview, Quaternary Sci Rev, 27, 1791-1828, 10.1016/j.quascirev.2008.06.013, 2008.
1016 Wanner, H., Mercolli, L., Grosjean, M., and Ritz, S. P.: Holocene climate variability and change; a
1017 data-based review, J Geol Soc London, 172, 254-263, 10.1144/jgs2013-101, 2015.
1018 Wanner, H., Solomina, O., Grosjean, M., Ritz, S. P., and Jetel, M.: Structure and origin of Holocene
1019 cold events, Quaternary Sci Rev, 30, 3109-3123, 10.1016/j.quascirev.2011.07.010, 2011.
1020 Weldeab, S., Lea, D. W., Schneider, R. R., and Andersen, N.: 155,000 Years of West African
1021 Monsoon and Ocean Thermal Evolution, Science, 316, 1303, 2007.
1022 Wiersma, A. P., and Renssen, H.: Model–data comparison for the 8.2kaBP event: confirmation of
1023 a forcing mechanism by catastrophic drainage of Laurentide Lakes, Quaternary Sci Rev, 25,
1024 63-88, http://dx.doi.org/10.1016/j.quascirev.2005.07.009, 2006.
1025 Wiersma, A. P., Roche, D. M., and Renssen, H.: Fingerprinting the 8.2 ka event climate response in
1026 a coupled climate model, J Quaternary Sci, 26, 118-127, 10.1002/jqs.1439, 2011.
1027 Zhang, H.-L., Yu, K.-F., Zhao, J.-X., Feng, Y.-X., Lin, Y.-S., Zhou, W., and Liu, G.-H.: East Asian Summer
1028 Monsoon variations in the past 12.5ka: High-resolution δ18O record from a precisely dated
1029 aragonite stalagmite in central China, J Asian Earth Sci, 73, 162-175, 2013.

1030 Zhang, H., Cai, Y., Tan, L., Qin, S., and An, Z.: Stable isotope composition alteration produced by
1031 the aragonite-to-calcite transformation in speleothems and implications for paleoclimate
1032 reconstructions, Sediment Geol, 309, 1-14, 2014.
1033 Zhang, R., and Delworth, T. L.: Simulated tropical response to a substantial weakening of the
1034 Atlantic thermohaline circulation, J Climate, 18, 1853-1860, Doi 10.1175/Jcli3460.1, 2005.
1035 Zinke, J., Dullo, W. C., Heiss, G. A., and Eisenhauer, A.: ENSO and Indian Ocean subtropical dipole
1036 variability is recorded in a coral record off southwest Madagascar for the period 1659 to
1037 1995, Earth Planet Sc Lett, 228, 177-194, 10.1016/j.epsl.2004.09.028, 2004.
1038 Zinke, T., Loveday, B. R., Reason, C. J. C., Dullo, W. C., and Kroon, D.: Madagascar corals track sea
1039 surface temperature variability in the Agulhas Current core region over the past 334 years,
1040 Sci Rep-Uk, 4, 1-8, 10.1038/srep04393, 2014.

Figures

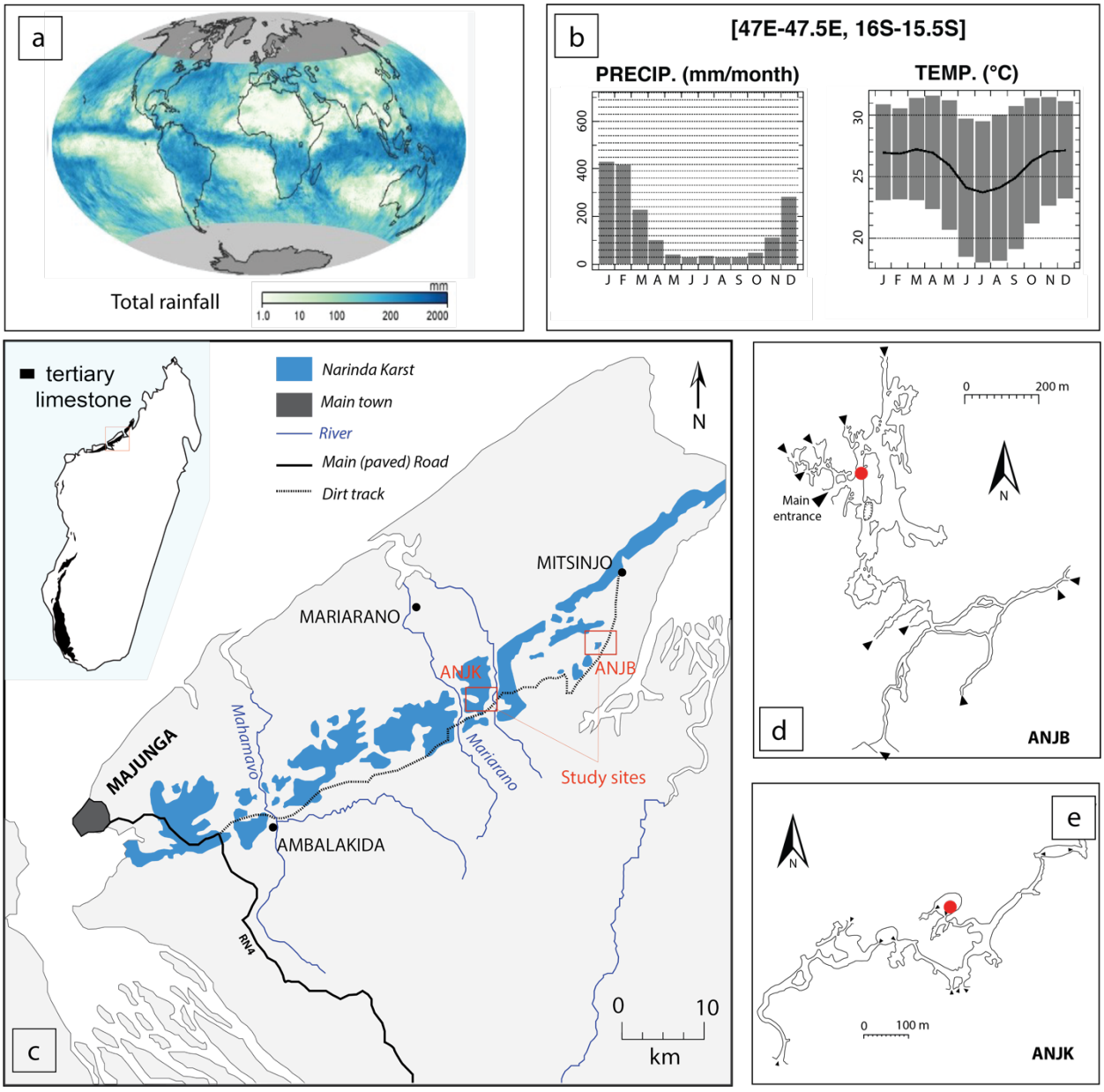

Figure 1: **Climatological and geographic setting of Madagascar and the study area**. (a) Global rainfall maps recorded by NASA's Tropical Rainfall Measuring Mission (TRMM) satellite showing the total monthly rainfall in millimeters and the overall position of the ITCZ during November, 2006. Darker shades of blue indicate regions of higher rainfall (source: NASA Earth Observatory, 2016). (b) Barplots of monthly precipitation, and monthly average of daily maximum, minimum, and mean temperature in NW Madagascar, based on 1971–2000 climate data. Source: http://iridl.ldeo.columbia.edu/ (accessed August 31, 2016). (c) Simplified map showing the

1050 southwest part of the Narinda karst and the location of the study areas. Inset figure is a map of
1051 Madagascar showing the extent of the Tertiary limestone outcrop that makes up the Narinda karst.
1052 (d-e) Maps of Anjohibe (ANJB) and Anjokipoty (ANJK) caves (St-Ours, 1959; Middleton and
1053 Middleton, 2002), with approximate location for sample collection (red dots). See Figs. S1–S3 for
1054 additional information about the study locations.
1055

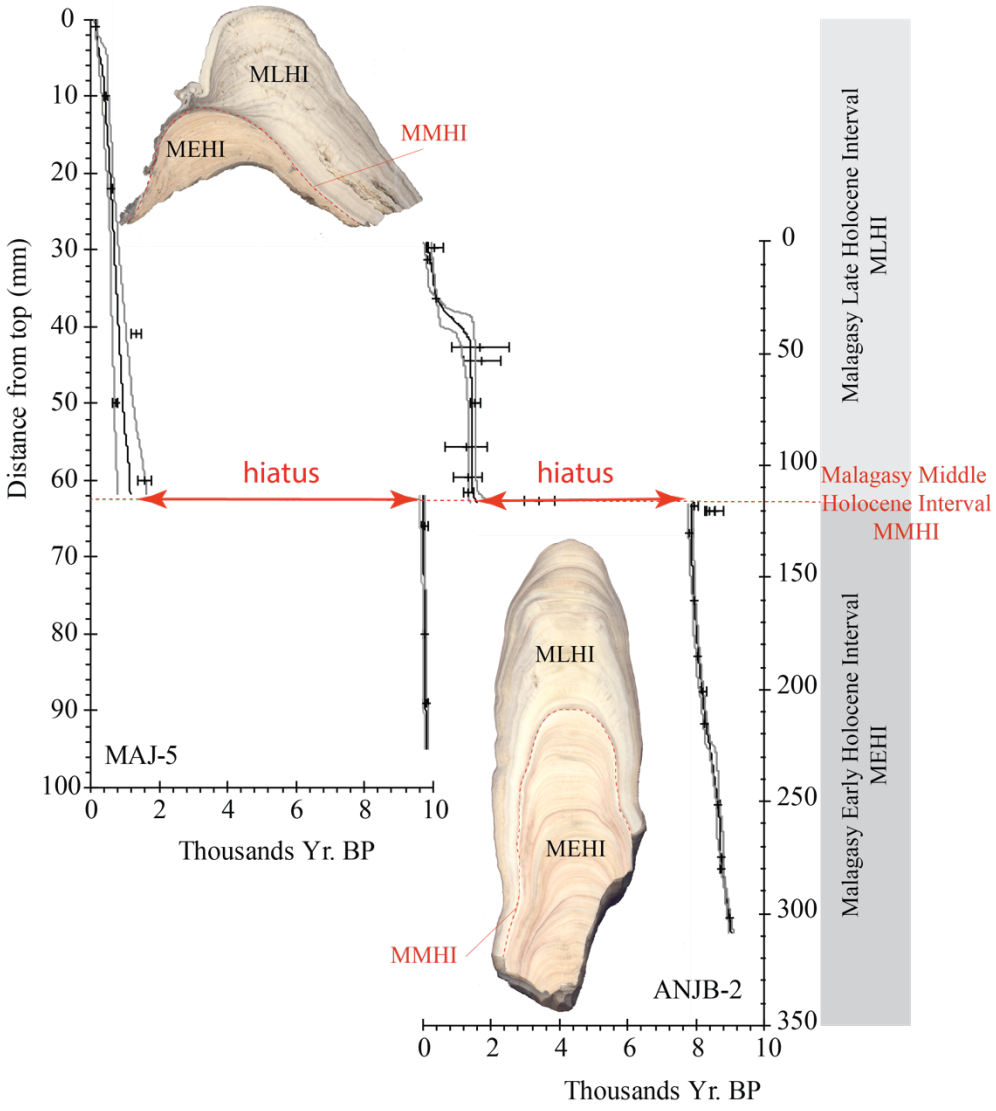

1056
1057 Figure 2: **Age model of Stalagmite MAJ-5 (left) and ANJB-2 (right)** using the StalAge1.0 algorithm
1058 of Scholz and Hoffman (2011) and Scholz et al. (2012). Scanned image of the two samples are
1059 shown for reference and to indicate the three distinct Holocene intervals.
1060

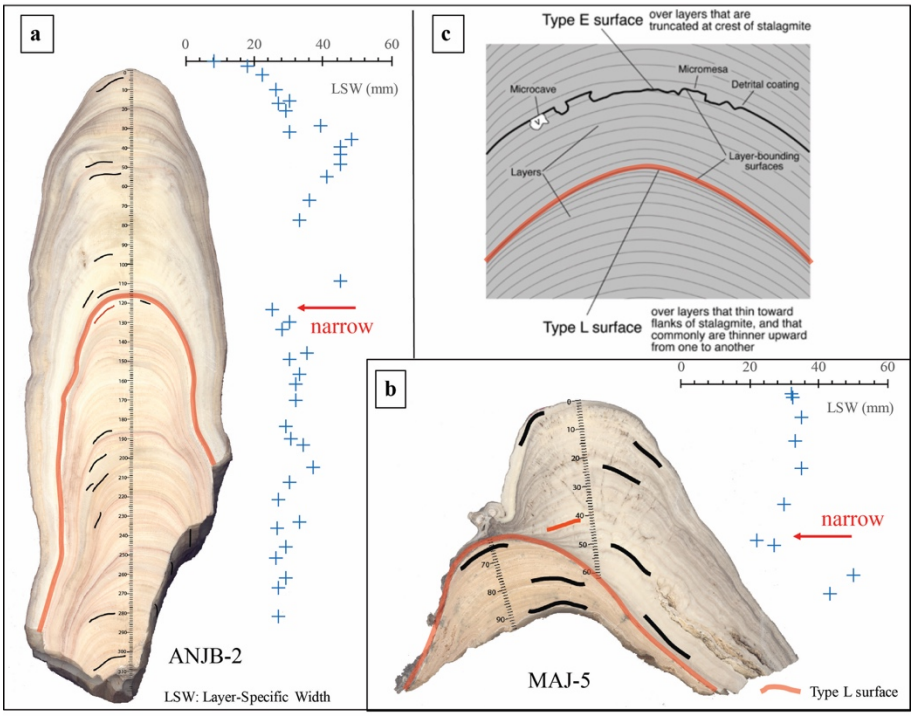

Figure 3: a) Scanned image of Stalagmite ANJB-2 and the corresponding variations in layer-specific width (LSW). b) Scanned image of Stalagmite MAJ-5 and the corresponding layer-specific width (LSW). c) Sketches of typical layer-bounding surfaces (Type E and Type L) of Railsback et al. (2013). Close-up photographs of the hiatuses are shown in Fig S6.

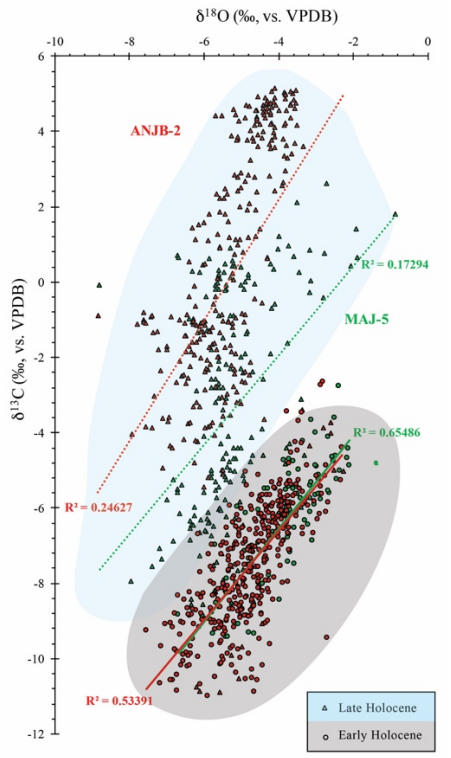

Figure 4: **Stable isotope data**. Scatterplots of $\delta^{13}C$ and $\delta^{18}O$ for Stalagmite MAJ-5 (green) and ANJB-2 (red) during the Malagasy early Holocene interval (circle) and the Malagasy late Holocene interval (triangle). The plot shows distinctive early and late Holocene conditions (roughly highlighted in gray and light blue, respectively).

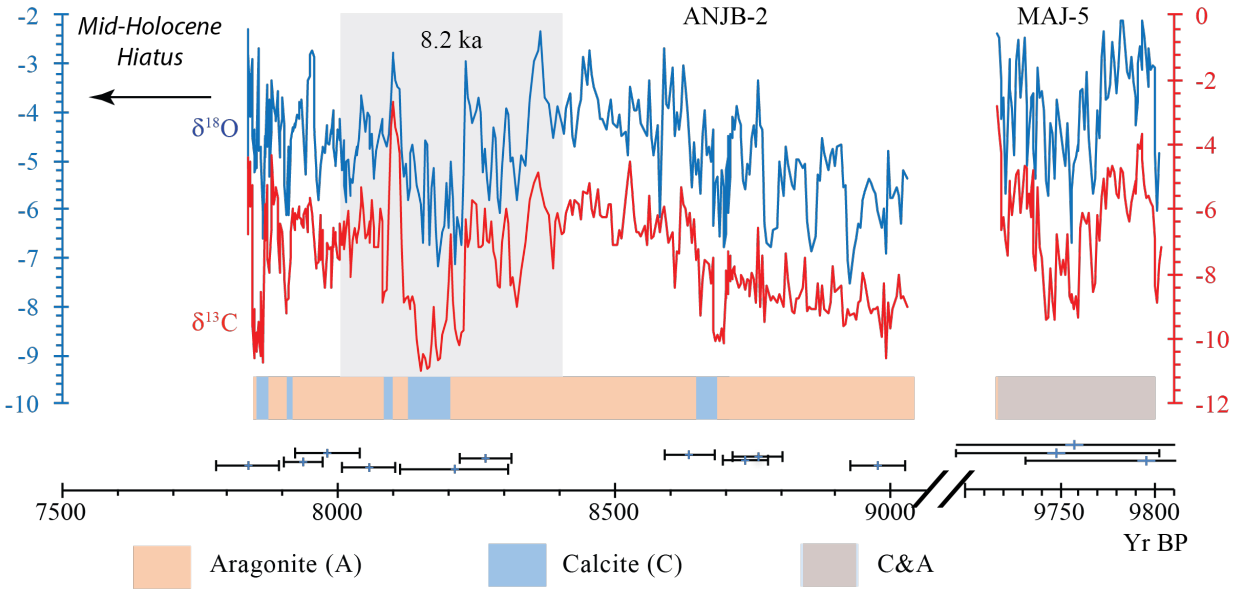

Figure 5: Variations in $\delta^{13}C$, $\delta^{18}O$, and mineralogy in Stalagmite ANJB-2 and Stalagmite MAJ-5 during the Malagasy Early Holocene Interval. Supplementary Fig. S6 shows both the corrected and uncorrected isotope values.

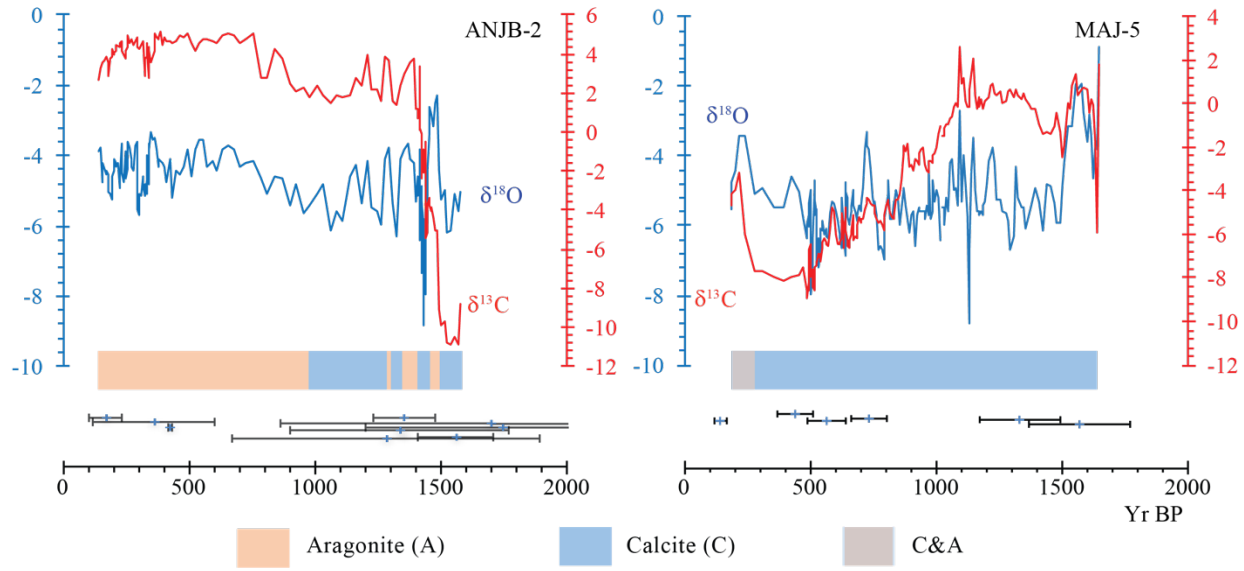

Figure 6: Variations in $\delta^{13}C$, $\delta^{18}O$, and mineralogy in Stalagmite ANJB-2 and Stalagmite MAJ-5 during the Malagasy Late Holocene Interval. Supplementary Fig. S7 shows both the corrected and uncorrected isotope values, and Fig. S8 compares the corrected $\delta^{18}O$ values for both stalagmites.

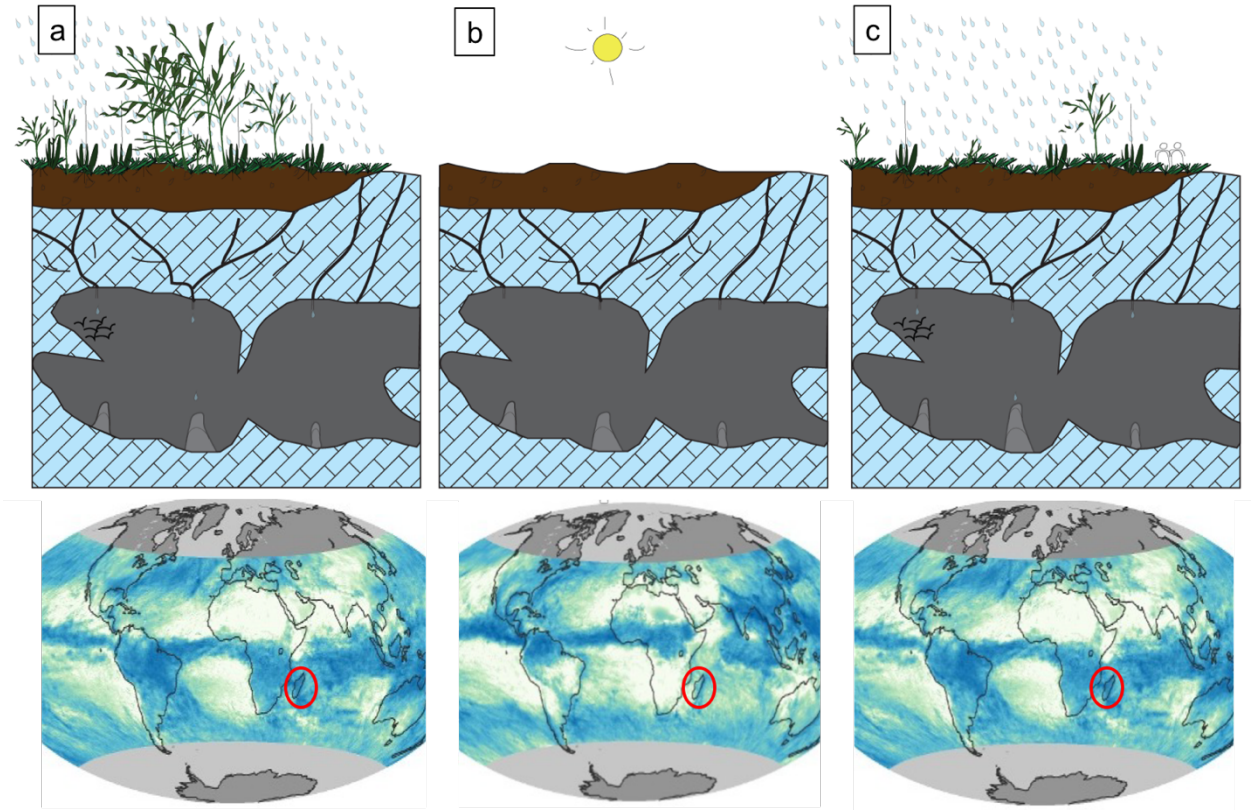

Figure 7: **Simplified models portraying Holocene climate change in NW Madagascar and the possible climatic conditions linked to the ITCZ**. a) Wetter conditions during the early Holocene with the ITCZ further south (prior to c 7.8 ka BP), favorable for stalagmite deposition. b) Periodic dry conditions during the mid-Holocene (between c. 7.8 and 1.6 ka BP) with the ITCZ further north leading to no stalagmite formation (refer to Sect. 5.2.2). c) Wetter conditions during the late Holocene (after c. 1.6 ka BP) with the ITCZ further south, favorable for stalagmite deposition. Drawings are not to scale. The bottom figures are from the same source as Fig. 1a, and they are only used here to give a perspective of the possible position of the ITCZ during the early, mid, and late Holocene. Madagascar is indicated with a red ellipse.

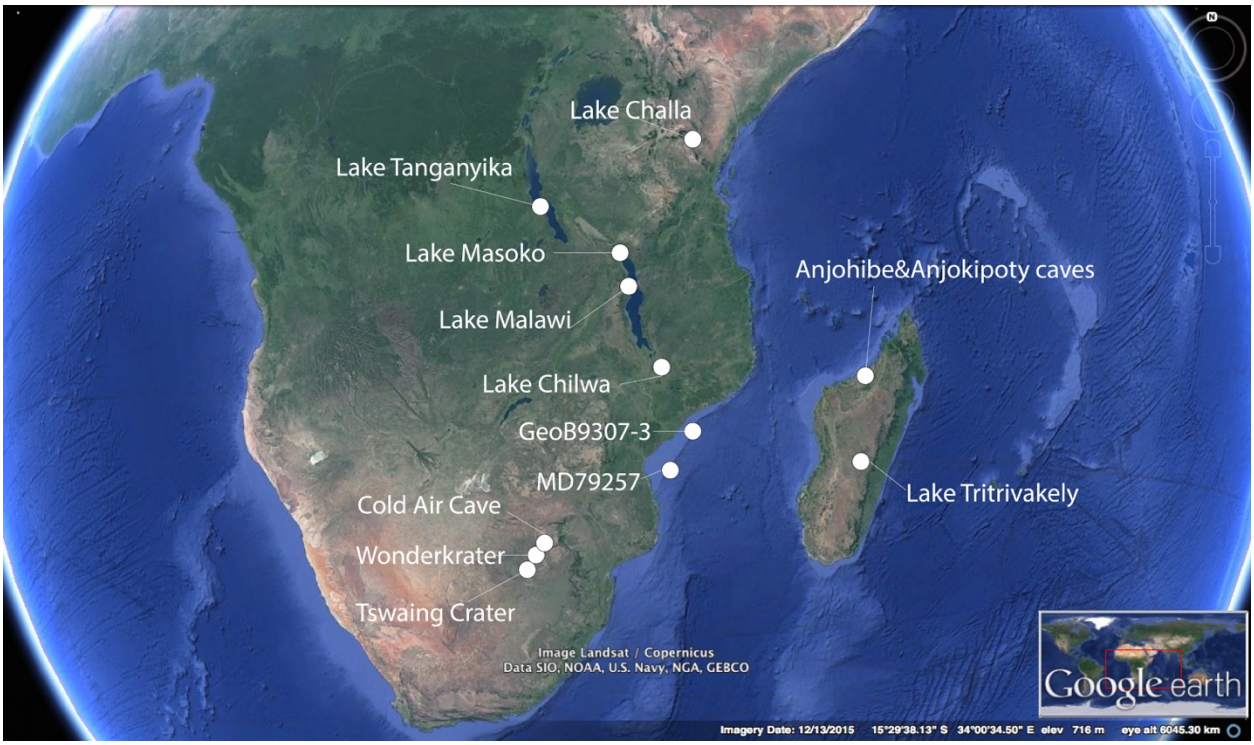

Figure 8: Regional comparison. Google Earth image showing the location of sites reported in Table S3 and in Figure 9. Most site records are from lake sediments, except for GeoB9307-3 (onshore off delta sediments), MD79257 (alkenone from marine sediment core), and Cold Air, Anjohibe, and Anjokipoty caves (stalagmites $\delta^{18}O$).

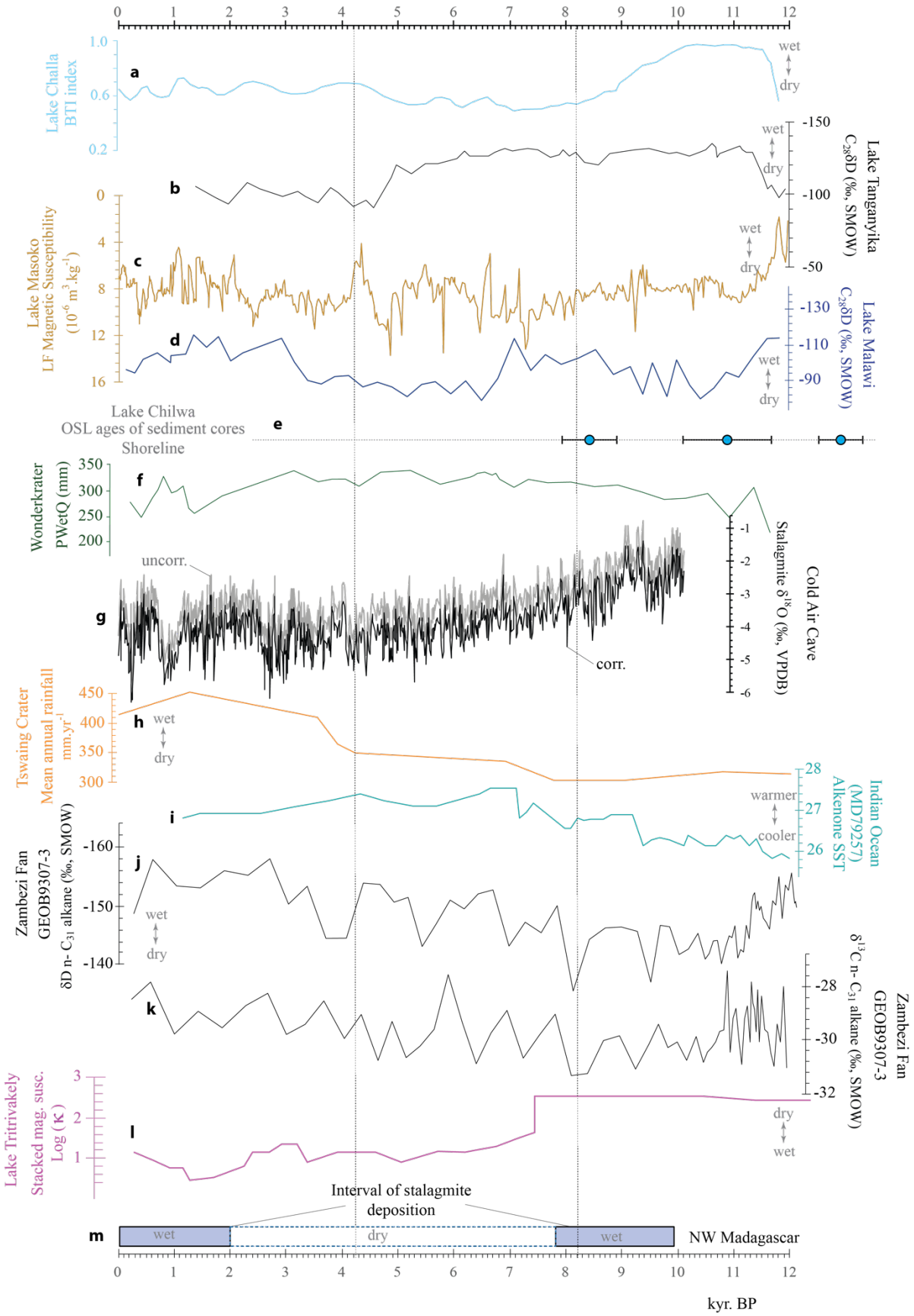
Lake Challa
BTI index
a
wet
dry
Lake Tanganyika
C28δD (‰, SMOW)
b
Lake Masoko
LF Magnetic Susceptibility
(10-6 m3.kg-1)
c
Lake Malawi
C28δD (‰, SMOW)
d
Lake Chilwa
OSL ages of sediment cores
Shoreline
e
Wonderkrater
PWetQ (mm)
f
uncorr.
corr.
Stalagmite δ18O (‰, VPDB)
Cold Air Cave
g
Tswaing Crater
Mean annual rainfall
mm.yr-1
h
warmer
cooler
Indian Ocean
(MD79257)
Alkenone SST
i
Zambezi Fan
GEOB9307-3
δD n- C31 alkane (‰, SMOW)
j
δ13C n- C31 alkane (‰, SMOW)
k
Lake Tritrivakely
Stacked mag. susc.
Log (κ)
l
Interval of stalagmite
deposition
m
NW Madagascar
kyr. BP

1108

Figure 9: Regional comparison. a) Lake Challa BTI index (Verschuren et al., 2009). b) Lake Tanganyika C_{28} δD (Tierney et al., 2008, 2010). c) Lake Masoko low field magnetic susceptibility ($10^{-6}.m^3kg^{-1}$) (Garcin et al., 2006). d) Lake Malawi C_{28} δD (Konecky et al., 2011). e) Lake Chilwa OSL dates of shoreline (Thomas et al., 2009). f) Wonderkrater reconstructed paleoprecipitation, PWetQ (Precipitation of the Wettest Quarter; Truc et al., 2013). g) Cold Air Cave corrected (corr.) and uncorrected (uncorr.) $\delta^{18}O$ profiles from Stalagmite T8 (Holmgren et al., 2003). h) Tswaing Crater paleo-rainfall derived from sediment composition (Partridge et al., 1997). i) Indian Ocean SST records from alkenone (Bard et al., 1997; Sonzogni et al., 1998). j-k) Zambezi δD n-C_{31} alkane $\delta^{13}C$ n-C_{31} alkane (Schefuß et al., 2011). l) Lake Tritrivakely stacked magnetic susceptibility (Williamson et al., 1998). m) NW Madagascar (Anjohibe and Anjokipoty) interval of deposition of Stalagmite ANJB-2 and Stalagmite MAJ-5 (this study). The two vertical dashed lines indicate the boundary of the Early, Middle, and Late Holocene by Walker et al. (2012) and Head and Gibbard (2015).

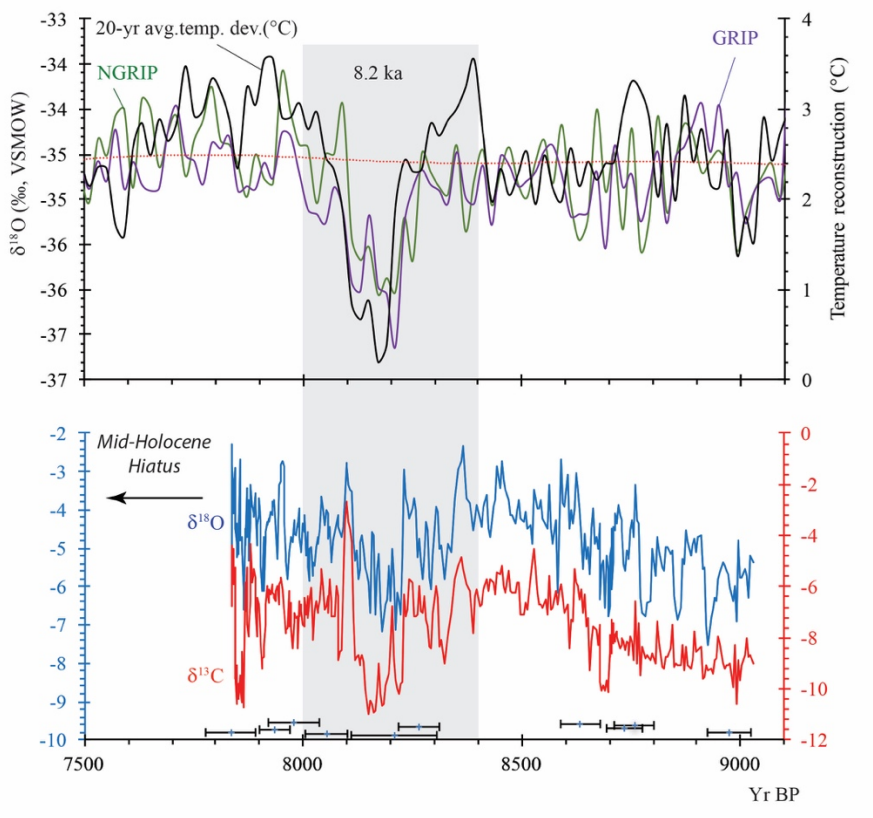

Figure 10: **The 8.2 ka BP event in Madagascar**. Oxygen isotope record from Greenland (GRIP and NGRIP) ice cores (Vinther et al., 2009) compared with Stalagmite ANJB-2 $\delta^{18}O$ and $\delta^{13}C$.